# ON SEISMIC WAVES.

(Fourth paper.)

By

**B. Gutenberg** and **C. F. Richter,**

Balch Graduate School of the Geological Sciences, California Institute of Technology, Pasadena.

Contribution No. 261.

(With 4 figures.)

## Contents.



**Zusammenfassung:** Die vorliegende Arbeit bildet den Schluß der Serie gleichen Namens. In ihr werden die Ergebnisse von Messungen an Seismogrammen von Beben mit tiefen Herden dazu benutzt, Laufzeitkurven einer Reihe von Phasen zu verbessern und daraus neue Werte für die Wellengeschwindigkeiten im Erdinnern abzuleiten. Dies geschieht zunächst für $P$, das keinerlei Verbesserung benötigt, und $S$. Die beobachteten Laufzeitkurven für die am Erdkern reflektierten Wellen $PcP$, $PcS$ und $ScS$ stimmen vorzüglich zu den aus den Wellengeschwindigkeiten berechneten. Um diese Geschwindigkeiten für die obersten 700 km zu prüfen, wurden die Steigzeiten (Herd-Epizentrum) von $P$ und $S$ verwandt, ferner die Zeitdifferenz $20^{m}\,14^{s}$ (Zeit für $P'$ entlang einem vollen Durchmesser) minus der Zeit von $P'$ zum Gegenpunkt für das betreffende Erdbeben mit tiefem Herd, ferner $^1/_2\,(pP' - P')$, und schließlich $15^{m}38^{s}$ — $ScS$ beobachtet nahe dem Epizentrum, wo die erstere Ziffer die Zeit angibt, die nach den Beobachtungen eine $ScS$-Welle braucht, die an der Erdoberfläche beginnt, vertikal nach unten läuft und nach Reflexion am Erdkern zur Ausgangsstelle zurückkehrt. Alle

beobachteten Werte stimmen mit den für $P$ bzw. $S$ berechneten Kurven vorzüglich überein (Fig. 1).

Aus den für $P'$ und $SKS$ gefundenen Laufzeitkurven wird sodann die Laufzeitkurve für Wellen, die an der Kernoberfläche beginnen und enden, abgeleitet. Hierbei wird der Brennpunkt von $SKS$ (Fig. 2) berücksichtigt sowie die Tatsache, daß die seither als „gebeugte $P'$-Welle" bezeichnete Phase manchmal so stark ist, daß sie nur als direkte Welle gedeutet werden kann (Fig. 4). Die Ergebnisse werden dazu benutzt, um Laufzeitkurven der wichtigeren durch den Kern gehenden Wellen zu berechnen. Die Übereinstimmung mit den beobachteten Laufzeiten ist durchweg sehr gut.

In Tabelle 37 werden außer den neuen Wellengeschwindigkeiten auch die Ergebnisse von Bullen über Dichte und Druck im Erdinnern zusammengestellt sowie die Werte für die elastischen Konstanten, die sich aus beiden Gruppen von Werten ergeben. Es besteht kein Grund zur Annahme, daß zwischen der unteren Grenzfläche der kontinentalen Schichten (Unstetigkeitsfläche von Mohorovičić) und dem Erdkern irgendeine Unstetigkeitsfläche erster Ordnung existiert.

Für alle wichtigeren Wellen sind Laufzeitkurven für einen Herd in der Erdoberfläche berechnet und mitgeteilt. Schließlich gibt Figur 3 einen Überblick über den ungefähren Verlauf der Strahlen und Wellenflächen im Erdinnern nach der vorliegenden Arbeit.

## I. Introductory.

This paper is in continuation of a series under the same title[1][2][3]. For convenience, these will be referred to in the text as "Seismic Waves I, II, III". These papers were based almost exclusively on the data of shocks at normal depth. It appeared probable that the use of observations of deep-focus earthquakes would lead to more precise determination of travel times, and of the velocities of seismic waves in the interior of the earth. We owe this opportunity to the exceptional sharpness of the recorded impulses from most such shocks, and to the freedom of the seismograms from disturbance by surface waves. The occurrence of such sharp seismograms was pointed out by Zoeppritz in a paper published posthumously in 1912.

Before deep-focus shocks can be used for such a purpose, detailed preliminary investigations are necessary, in order to develop precise methods for the determination of epicenter, depth, and origin time. Such methods have been published in two recent papers[4] [5], which will be referred to as "Materials I, II." In order to make certain that no valuable data would be overlooked, a revised catalogue of deep-focus shocks was constructed[6]. Serial numbers attached to shocks in the present paper refer to this catalogue.

## II. Longitudinal waves in the mantle ($P$).

The travel times of $P$ for the better recorded shocks of our deep-focus catalogue have been compared with the calculated times tabulated in "Materials" I and II. These were derived from the data of normal shocks as given in "Seismic Waves" I and II. The residuals of $P$ with respect to these tables rarely exceed a few seconds, and remain within the limits of error.

As pointed out by JEFFREYS[7]) our travel times[1]) for $P$ agree closely with his, the difference generally being within two seconds, and at most distances within one second. This is true, except for a small additive constant. As may be seen by comparison with JEFFREYS' recent travel times for surface focus[8]), the apparent close agreement obtains between those times and the times which we have given for "normal" depth of focus.

To reduce the travel times of $P_n$ for shocks at normal depth to those for surface focus (zero focal depth), the following correction should be added — assuming that the given focus is in the granitic layer and that there are no overlying sediments:

$$C = h\left(\frac{1}{v \cos i} - \frac{\tan i}{\overline{v}}\right)$$

where $v$ is the velocity in the granitic layer, $\overline{v}$ is the apparent velocity of $P_n$ at the surface, and $i$ is the angle of incidence at the surface. Here the first term is the travel time from the surface down to depth $h$; the second term is due to the change in distance. For short distances we may assume $\sin i = 5.6/7.9$ and $\overline{v} = 7.9$, $v = 5.6$; whence $C = 0.12\,h$.

This correction can best be determined for regions such as Southern California, where travel times, depths, and structures have been worked out[9]). In this area the times of $P_n$ are given by

$$P_n = 5.8 + \Delta/7.9.$$

This corresponds to the focal depth which is normal for the Southern California region (about 15 km.). Hence for zero focal depth in this region the constant term should be increased to $5.8 + 0.12 \times 15 = 7.6$ sec. In the Long Beach earthquake for which $h$ was about 10 km., a travel time of 56 seconds was observed at a distance of $3.5°$; this gives a travel time of 57.2 sec. for zero depth, making the constant term 8.2 sec. Considering that the upper layers in California are relatively thin, a constant term of 9 seconds has been used as generally representative, and Table 1 for zero focal depth has been constructed on this basis.

Table 1.

Travel times $t$ (min:sec) of $P$ for zero focal depth, reciprocals $1/\bar{v}$ of the apparent velocities for the arcs beginning and ending at a depth of 40 km (sec/km), and sine of the angle of incidence $i_S$ at the core of a transverse wave which has the same apparent velocity as $P$ at a depth of 40 km.

| Dist. | $t$ | $1/\bar{v}$ | Dist. | $t$ | $1/\bar{v}$ | sin $i_S$ | Dist. | $t$ | $1/\bar{v}$ | sin $i_S$ |
|---|---|---|---|---|---|---|---|---|---|---|
| 1° | (0:23) | 0.127 | 36° | 7:06 | 0.076 | | 71° | 11:24 | 0.054 | 0.719 |
| 2 | 37 | 127 | 37 | 15 | 755 | | 72 | 30 | 53 | 705 |
| 3 | 51 | 127 | 38 | 24 | 755 | | 73 | 35 | 52 | 692 |
| 4 | 1:05 | 127 | 39 | 33 | 755 | | 74 | 41 | 51 | 679 |
| 5 | 19 | 127 | 40 | 41 | 755 | | 75 | 46 | 50 | 666 |
| 6 | 33 | 127 | 41 | 50 | 755 | | 76 | 52 | 49 | 652 |
| 7 | 47 | 127 | 42 | 58 | 755 | | 77 | 58 | 49 | 651 |
| 8 | 2:01 | 127 | 43 | 8:07 | 75 | 0.998 | 78 | 12:04 | 49 | 648 |
| 9 | 15 | 127 | 44 | 15 | 74 | 985 | 79 | 10 | 485 | 646 |
| 10 | 29 | 127 | 45 | 23 | 725 | 965 | 80 | 15 | 48 | 639 |
| 11 | 43 | 127 | 46 | 30 | 71 | 945 | 81 | 20 | 47 | 626 |
| 12 | 57 | 127 | 47 | 37 | 70 | 932 | 82 | 25 | 46 | 612 |
| 13 | 3:11 | 126 | 48 | 45 | 68 | 905 | 83 | 30 | 455 | 606 |
| 14 | 25 | 125 | 49 | 53 | 675 | 898 | 84 | 35 | 45 | 600 |
| 15 | 38 | 116 | 50 | 9:00 | 665 | 885 | 85 | 40 | 45 | 599 |
| 16 | 51 | 108 | 51 | 07 | 66 | 878 | 86 | 45 | 45 | 597 |
| 17 | 4:04 | 104 | 52 | 14 | 655 | 872 | 87 | 50 | 445 | 594 |
| 18 | 16 | 101 | 53 | 22 | 65 | 865 | 88 | 55 | 445 | 590 |
| 19 | 28 | 099 | 54 | 29 | 65 | 863 | 89 | 13:00 | 44 | 586 |
| 20 | 39 | 096 | 55 | 36 | 645 | 858 | 90 | 05 | 435 | 579 |
| 21 | 49 | 94 | 56 | 43 | 64 | 852 | 91 | 10 | 425 | 566 |
| 22 | 5:00 | 92 | 57 | 51 | 635 | 845 | 92 | 14 | 415 | 552 |
| 23 | 10 | 89 | 58 | 59 | 635 | 843 | 93 | 18 | 41 | 546 |
| 24 | 19 | 87 | 59 | 10:06 | 63 | 841 | 94 | 23 | 40 | 534 |
| 25 | 29 | 86 | 60 | 13 | 63 | 837 | 95 | 27 | 40 | 532 |
| 26 | 38 | 84 | 61 | 20 | 625 | 832 | 96 | 32 | 40 | 532 |
| 27 | 47 | 825 | 62 | 27 | 62 | 825 | 97 | 35 | 399 | 531 |
| 28 | 55 | 81 | 63 | 33 | 615 | 819 | 98 | 40 | 399 | 531 |
| 29 | 6:04 | 80 | 64 | 40 | 61 | 812 | 99 | 45 | 398 | 530 |
| 30 | 13 | 79 | 65 | 47 | 605 | 805 | 100 | 50 | 398 | 529 |
| 31 | 21 | 78 | 66 | 53 | 595 | 792 | 101 | 54 | 397 | 528 |
| 32 | 30 | 775 | 67 | 11:00 | 58 | 772 | 102 | 58 | 396 | 527 |
| 33 | 39 | 77 | 68 | 06 | 575 | 765 | 103 | 14:03 | 396 | 527 |
| 34 | 48 | 765 | 69 | 12 | 57 | 759 | | | | |
| 35 | 57 | 76 | 70 | 18 | 555 | 739 | | | | |

The times of Table 1 are consequently about 3 seconds later than those given by Jeffreys for surface focus, since he has used a constant term of 6 seconds. This difference arises from a difference in interpretation as to the depth of the Central European earthquakes, which Jeffreys supposes to have originated only a few kilometers from the surface. His use of these results has the effect of assuming that all normal earthquakes originate close to the surface.

There is an outstanding uncertainty in accounting for the observations of waves emerging at epicentral distances near 20°. (For details, and selected observations, refer to Section X of Seismic Waves II.) The observed times definitely establish that the increase in velocity with depth, $dv/dh$, has a maximum at a depth between 250 and 500 km. It is still a moot point whether $dv/dh$ is discontinuous at this depth, or whether, if continuous, the derivative is large enough to produce cusps in the travel time curve.

As Jeffreys has pointed out[10]) the differences in expected travel times under the several assumptions are too small to make a decision on this basis possible. This is confirmed by observations at the California stations. We have previously given data chiefly for Mexican shocks; the occurrence of recent shocks in the Queen Charlotte Islands has given further confirmation. In all these instances the amplitudes remain relatively large in the whole range near 20°, with no sign of a rapid change in amplitude such as should occur if the travel-time curve has a cusp. Moreover, the Californian records show nothing identifiable as the second branch of such a curve (Jeffreys' $P_d$ following $P_r$). Certain records show a large impulse about 7 seconds following $P$ at a distance of about 21°; but this appears too late to be $P_d$, and may even be $pP$.

Under these circumstances the writers still conclude that the velocity probably increases continuously at the corresponding critical depth. There is no unimpeachable evidence of any first-order discontinuity between the Mohorovičić discontinuity and the core.

Table 1 presents revised travel times of $P$ for zero focal depth. The previous results for normal earthquakes have been verified and slightly modified in consequence of the work with deep shocks. It is believed that the times given are the best obtainable with the data now in hand. The times refer to average or usual conditions; focus and observing stations are supposed to be located in continental areas remote from exceptional crustal structures (no thick sediments, average thickness of continental layers). With this restriction the times are probably correct to within two seconds.

The table includes other quantities for use in calculation; the value of sin $i_S$ is important in finding the travel times of core waves reflected and transformed at the surface, such as *PSKS.*

## III. Transverse waves in the mantle (*S*).

The problem of the propagation of transverse waves in the mantle is rendered more difficult by the circumstance that a small beginning of the *S* group is often obscured by preceding seismic motion. For this reason it has been the practice in recent investigations to use the earliest reliable readings of *S*, even when the later motion is much larger. However, there is a possible source of error in this procedure, as waves which are transverse over most of their path may be longitudinal within the crust, either near the source or near the observing station; the transformation between longitudinal and transverse waves may take place

Table 2.

Residuals (seconds) of *S*-waves in deep focus earthquakes.

| | Serial numbers of Shocks | | | | | | | | | |
|---|---|---|---|---|---|---|---|---|---|---|
| | 26; 136<br>143; 150<br>159 | 234<br>240<br>241 | 16; 17<br>246/49 | 48<br>July 25.<br>1932 | 83<br>170<br>309 | 181/3<br>186 | 104<br>192 | 40; 57<br>64; 107<br>114; 221 | 29/31<br>40; 109<br>132 | Assumed for zero depth |
| Dist. degr. | Average depth of focus in km | | | | | | | | | |
| | 150 | 220 | 230 | 300 | 350 | 400 | 400 | 600 | 650 | |
| 52 | —3 | | —5 | | —5 | | | —7 | —5 | —5 |
| 30 | — ? | | —4 | | —5 | | | —7 | —6 | —5 |
| 35 | — ? | | 0 | | —5 | | | — ? | —5. | —5 |
| 40 | —1 | —3 | 0 | | —5 | | —2 | —3 | —3 | —3 |
| 45 | —3 | —2 | 2 | | —6 | | 1 | —3 | —3 | —3 |
| 50 | —4 | 0 | 6 | | —6 | | 2 | —3 | —5 | —3 |
| 55 | —4 | 6 | 4 | | —1 | —1 | 3 | —3 | —8! | —3 |
| 60 | —5 | 3 | 1 | | 1 | —3 | 0 | —4 | —6 | —4 |
| 65 | —4 | 3 | | | 2 | —1 | | —2 | | —2 |
| 70 | 1 | 4 | 7 | 3 | 7 | 3 | 3 | —1 | —1 | 0 |
| 75 | —1 | | 6 | 3 | 3 | —2 | 5 | —2 | —2 | —2 |
| 80 | —1 | 10 | 0 | 2 | —1 | —3 | 4 | 0 | —2 | —2 |
| 85 | —2 | 6 | 0 | 1 | 0 | —4 | 3 | —2 | —3 | —3 |
| 90 | —6 | 2 | —2 | | —3 | —4 | 2 | | —5 | —4 |
| 95 | —3 | —2 | 0 | | 0 | | 1 | | —4 | —3 |
| 100 | —1 | —1 | | | —1 | —3 | | | —2 | —2 |

at the Mohorovičić discontinuity or at some other level within the crust. Such waves should arrive a few seconds earlier than the true $S$. This error is diminished in deep-focus earthquakes, since the change in wave-type can only occur at one end of the path. Moreover, the $S$ phase is usually very sharp in deep shocks. Accordingly, the travel times of $S$ have been examined for 37 such shocks.

The results are summarized in Table 2, which gives residuals with respect to the $S$ travel times in Table 15 of "Materials I." Epicenters, origin times, and serial numbers of the shocks, are those given in our catalogue[6]). The distances in the first column of the present table are reduced to zero depth from the actually larger distances of the observing stations. The residuals in Table 2 are averages of the earliest readings for each distance group. The final results, in the last column, may still be affected by systematic errors amounting to a few seconds. The

Table 3.

Travel times of $S$-waves (min:sec). A: Assumed for zero depth; the travel time tables for larger depths[4]) have been based on these values; B: observed residuals (last column in table 2); $C$ corrected times $A+B$; $D$ difference $C$ minus the values given by Jeffreys[8]) for a continental surface focus; E: travel times for focus and arrival at a depth of 40 km, corresponding to the values $C$.

| Dist. degr. | $A$ | $B$ | $C$ | $D$ | $E$ |
|---|---|---|---|---|---|
| 15 | 6:28 | (—4) | 6:24 | —2 | 6:08 |
| 20 | 8:22 | (—6) | 8:16 | —3 | 7:58 |
| 25 | 9:55 | —5 | 9:50 | 0 | 9:31 |
| 30 | 11:15 | —5 | 11:10 | 0 | 10:51 |
| 35 | 12:32 | —5 | 12:27 | —1½ | 12:08 |
| 40 | 13:46 | —3 | 13:43 | —1½ | 13:24 |
| 45 | 14:59 | —3 | 14:56 | —2 | 14:36 |
| 50 | 16:09 | —3 | 16:06 | —3½ | 15:46 |
| 55 | 17:20 | —3 | 17:17 | —1 | 17:57 |
| 60 | 18:26 | —4 | 18:22 | —1 | 18:02 |
| 65 | 19:27 | —2 | 19:25 | —1 | 19:04 |
| 70 | 20:21 | —0 | 20:21 | —6 | 20:00 |
| 75 | 21:17 | —2 | 21:15 | —9 | 20:54 |
| 80 | 22:12 | —2 | 22:10 | —8 | 21:49 |
| 85 | 23:06 | —3 | 23:03 | —6 | 22:42 |
| 90 | 23:58 | —4 | 23:54 | —2 | 23:33 |
| 95 | 24:43 | —3 | 24:40 | 1 | 24:19 |
| 100 | 25:25 | —2 | 25:23 | 1½ | 25:02 |
| 105 | 26:06 | (—2) | 26:04 | 1 | 25:43 |

dispersion of the observations is especially large at distances of 70° to 80°, where $S$ is very small and shows much multiplicity, even without considering the many late readings referable to $ScS$, $SKS$ etc.

In Table 3, column A gives the travel times for zero focal depth, on which the deep-focus tables of our previous papers were based. The corresponding correction, determined in the last column of Table 2, here appear in column B; they are applied to give the corrected values in column C. Column D makes the comparison with values tabulated by JEFFREYS[8]) for a continental surface focus. Except for the interval from 70° to 85°, where our times are 6 to 9 seconds earlier than

Table 4.

Travel times $t$ in min.:sec and reciprocals of the apparent velocity in sec/degr. for $S$-waves starting and arriving at a depth of 40 km.

| Dist. degr. | $t$ | $1/v$ | Dist. degr. | $t$ | $1/v$ |
|---|---|---|---|---|---|
| | | 24.7 | | | |
| 2 | 0:49 | | 52 | 16:15 | |
| | | 24.7 | | | 13.6 |
| 4 | 1:39 | | 54 | 16:42 | |
| | | 24.7 | | | 13.4 |
| 6 | 2:28 | | 56 | 17:09 | |
| | | 24.6 | | | 13.2 |
| 8 | 3:17 | | 58 | 17:36 | |
| | | 24.6 | | | 13.0 |
| 10 | 4:07 | | 60 | 18:02 | |
| | | 24.6 | | | 12.5 |
| 12 | 4:56 | | 62 | 18:27 | |
| | | 24.5 | | | 12.0 |
| 14 | 5:45 | | 64 | 18:51 | |
| | | 23.0 | | | 11.7 |
| 16 | 6:31 | | 66 | 19:14 | |
| | | 21.7 | | | 11.4 |
| 18 | 7:14 | | 68 | 19:37 | |
| | | 20.7 | | | 11.0 |
| 20 | 7:56 | | 70 | 19:59 | |
| | | 19.5 | | | 10.9 |
| 22 | 8:35 | | 72 | 20:21 | |
| | | 18.1 | | | 10.9 |
| 24 | 9:11 | | 74 | 20:42 | |
| | | 17.0 | | | 10.9 |
| 26 | 9:45 | | 76 | 21:04 | |
| | | 16.7 | | | 10.9 |
| 28 | 10:18 | | 78 | 21:26 | |
| | | 16.3 | | | 10.9 |
| 30 | 10:51 | | 80 | 21:48 | |
| | | 15.6 | | | 10.8 |
| 32 | 11:22 | | 82 | 22:09 | |
| | | 15.4 | | | 10.7 |
| 34 | 11:53 | | 84 | 22:31 | |
| | | 15.2 | | | 10.5 |
| 36 | 12:23 | | 86 | 22:52 | |
| | | 15.0 | | | 10.3 |
| 38 | 12:53 | | 88 | 23:13 | |
| | | 14.8 | | | 10.1 |
| 40 | 13:23 | | 90 | 23:33 | |
| | | 14.7 | | | 9.8 |
| 42 | 13:52 | | 92 | 23:52 | |
| | | 14.7 | | | 9.3 |
| 44 | 14:22 | | 94 | 24:11 | |
| | | 14.6 | | | 8.7 |
| 46 | 14:51 | | 96 | 24:28 | |
| | | 14.3 | | | 8.5 |
| 48 | 15:20 | | 98 | 24:45 | |
| | | 13.9 | | | 8.4 |
| 50 | 15:48 | | 100 | 25:02 | |
| | | 13.7 | | | 8.3 |
| | | | 102 | 25:19 | |
| | | | | | 8.3 |

Jeffreys', the agreement is within 3 seconds. The larger differences cited by Jeffreys[8]) were due to comparing his times for surface focus with ours for normal depth. Column E gives travel times between two points 40 km. below the surface, calculated from the data in column C. Corrections for use in the transition from the 40 km. level to the surface are given in Table 5. The smoothed travel time curve for $S$ is given

Table 5.

Corrections in seconds to be added to the travel times of $S$ for the 40 km level to find the travel times for $S$ from a surface focus to the surface $\left(22/\cos i_{av} - \frac{0.72}{v} \tan i_{av}\right)$.

| Distance in degr. | 15 | 20 | 30 | 40 | 50 | 60 | >60 |
|---|---|---|---|---|---|---|---|
| Correction | 16 | 18 | 19 | 19 | 20 | 20 | 21 |

in Table 4, which also contains the reciprocals of the apparent velocity at the 40 km. level. Between 6° and 16° the data are based mainly on interpolation. The velocities of transverse waves in the mantle, calculated from the data of Table 4, appear in Table 6.

The following formulae have been used:

$$\log r = 3.80113 - 0.0024127 \int \cosh q \; d\theta$$

where $r$ is the radius vector of the deepest point reached, in kilometers, $q$ is the ratio of apparent velocities, and $\theta$ is measured in degrees. The

Table 6.

Velocity of transverse waves in the mantle of the earth as a function of the depth, and reciprocals which have been used in calculations.

| Depth km | $v$ km/sec | $1/v$ sec/km | Depth km | $v$ km/sec | $1/v$ sec/km |
|---|---|---|---|---|---|
| 0 | 3.2 | 0.312 | 600 | 5.6 | 0.178 |
| 10 | 3.3 | 303 | 700 | 5.9 | 170 |
| 20 | 3.4 | 294 | 900 | 6.3 | 159 |
| 30 | 3.7 | 270 | 1000 | 6.4 | 157 |
| 40 | 4.2 | 238 | 1200 | 6.5 | 153 |
| 50 | 4.4 | 225 | 1600 | 6.8 | 148 |
| 60 | 4.5 | 222 | 1800 | 6.9 | 144 |
| 100 | 4.5 | 222 | 2000 | 7.0 | 142 |
| 200 | 4.6 | 218 | 2100 | 7.0 | 142 |
| 300 | 4.8 | 209 | 2200 | 7.0 | 143 |
| 400 | 5.1 | 198 | 2300 | 7.0 | 142 |
| 500 | 5.3 | 187 | 2700 | 7.2 | 139 |
| | | | 2920 | 7.25 | 138 |

velocity at the corresponding depth is

$v = 0.017453\, r\bar{v}$, if the apparent velocity $\bar{v}$ is measured in degrees per second, or

$v = r\bar{v}/6326$ if measured in kilometers per second.

## IV. *PcP*, *ScP*. *PcS*, *ScS*.

From the velocities of $P$ as given in Table 18 of "Seismic Waves II" and those of $S$ in Table 6 of the present paper, we may calculate the travel times and angular distances of $P$ and $S$ passing between the surface of the earth and that of the core, using the formulae:

$$\theta = \int \frac{\tan i}{r}\, dr \qquad t = \int \frac{dr}{v \cos i}$$

$$\sin i = C \sin i_c \qquad C = \frac{v\, r_c}{r\, v_c}.$$

Here $i_c$ is the angle of incidence at the surface of the core, and $r_c$, $v_c$ are the corresponding radius and velocity. We have used $r_c = 3446$ km., and $v_c = 13.7$ km./sec. for longitudinal waves, $v_c = 7.25$ km./sec. for transverse waves.

The results are given in Table 7. The travel time curves for $PcP$ and $ScS$ from a surface focus can be taken directly from Table 7 by doubling the angular distances and times. To calculate the curve for $ScP$ or $PcS$ (the two are identical for zero focal depth), the quantities in Table 7 must be combined in such a way that the two values of $\sin i_c$ for longitudinal and transverse waves are in the ratio of the corresponding velocities; so that $\sin i_c$ for $S$ is 0.5292 times $\sin i_c$ for $P$.

Table 7.

Travel times ($t_P$ and $t_S$) and angular distances ($\theta_P$ and $\theta_S$) for paths between the surface of the earth and the surface of the core for longitudinal and transverse waves as a function of the sine of the respective angle of incidence at the surface of the core ($i_c$).

| $\sin i_c$ | $\theta_P$ degr. | $t_P$ min:sec | $\theta_S$ degr. | $t_S$ min:sec | $\sin i_c$ | $\theta_P$ degr. | $t_P$ min:sec | $\theta_S$ degr. | $t_S$ min:sec |
|---|---|---|---|---|---|---|---|---|---|
| | | | | | 0.56 | 14.5 | 4:37 | 14.9 | 8:27 |
| 0.00 | 0.0 | 4:17 | 0.0 | 7:50 | 57 | 14.8 | 38 | 15.2 | 28 |
| 05 | 1.2 | 18 | 1.2 | 51 | 58 | 15.1 | 38 | 15.5 | 30 |
| 10 | 2.3 | 18 | 2.4 | 51 | 59 | 15.4 | 39 | 15.9 | 32 |
| 15 | 3.5 | 19 | 3.7 | 52 | 60 | 15.8 | 40 | 16.2 | 34 |

Tabelle 7 (Continued).

| $\sin i_c$ | $\theta_P$ degr. | $t_P$ min : sec | $\theta_S$ degr. | $t_S$ min : sec | $\sin i_c$ | $\theta_P$ degr. | $t_P$ min : sec | $\theta_S$ degr. | $t_S$ min : sec |
|---|---|---|---|---|---|---|---|---|---|
| 16 | 3.8 | 19 | 3.9 | 52 | 61 | 16.2 | 41 | 16.6 | 36 |
| 17 | 4.0 | 19 | 4.2 | 53 | 62 | 16.5 | 42 | 16.9 | 38 |
| 18 | 4.3 | 19 | 4.4 | 53 | 63 | 16.9 | 43 | 17.3 | 40 |
| 19 | 4.5 | 20 | 4.7 | 54 | 64 | 17.3 | 44 | 17.7 | 42 |
| 20 | 4.8 | 20 | 4.9 | 54 | 65 | 17.6 | 45 | 18.0 | 44 |
| 21 | 5.0 | 20 | 5.2 | 55 | 66 | 18.0 | 46 | 18.4 | 46 |
| 22 | 5.3 | 20 | 5.4 | 55 | 67 | 18.4 | 47 | 18.8 | 48 |
| 23 | 5.5 | 20 | 5.7 | 55 | 68 | 18.8 | 48 | 19.2 | 50 |
| 24 | 5.7 | 21 | 5.9 | 56 | 69 | 19.2 | 49 | 19.6 | 52 |
| 25 | 6.0 | 21 | 6.2 | 56 | 70 | 19.6 | 50 | 20.1 | 54 |
| 26 | 6.2 | 21 | 6.4 | 57 | 71 | 20.0 | 52 | 20.5 | 56 |
| 27 | 6.5 | 21 | 6.7 | 57 | 72 | 20.4 | 53 | 21.0 | 8:59 |
| 28 | 6.7 | 22 | 6.9 | 58 | 73 | 20.9 | 54 | 21.4 | 9:01 |
| 29 | 7.0 | 22 | 7.2 | 58 | 74 | 21.3 | 56 | 21.8 | 04 |
| 30 | 7.3 | 22 | 7.4 | 59 | 75 | 21.7 | 57 | 22.3 | 07 |
| 31 | 7.5 | 22 | 7.7 | 8:00 | 76 | 22.2 | 4:59 | 22.8 | 10 |
| 32 | 7.8 | 23 | 8.0 | 01 | 77 | 22.7 | 5:01 | 23.3 | 13 |
| 33 | 8.1 | 23 | 8.2 | 02 | 78 | 23.2 | 03 | 23.8 | 16 |
| 34 | 8.3 | 24 | 8.5 | 03 | 79 | 23.7 | 04 | 24.4 | 19 |
| 35 | 8.6 | 24 | 8.8 | 04 | 80 | 24.3 | 06 | 24.9 | 23 |
| 36 | 8.8 | 25 | 9.0 | 05 | 81 | 24.8 | 08 | 25.4 | 27 |
| 37 | 9.1 | 25 | 9.3 | 05 | 82 | 25.4 | 10 | 26.0 | 31 |
| 38 | 9.4 | 26 | 9.6 | 06 | 83 | 26.0 | 12 | 26.6 | 35 |
| 39 | 9.6 | 26 | 9.8 | 07 | 84 | 26.6 | 14 | 27.2 | 39 |
| 40 | 9.9 | 27 | 10.1 | 08 | 85 | 27.3 | 16 | 27.9 | 43 |
| 41 | 10.1 | 27 | 10.4 | 09 | 86 | 27.9 | 19 | 28.6 | 48 |
| 42 | 10.4 | 28 | 10.6 | 10 | 87 | 28.6 | 22 | 29.4 | 54 |
| 43 | 10.7 | 28 | 10.9 | 11 | 88 | 29.4 | 25 | 30.2 | 9:59 |
| 44 | 11.0 | 29 | 11.2 | 12 | 89 | 30.3 | 29 | 31.0 | 10:06 |
| 45 | 11.3 | 29 | 11.5 | 13 | 90 | 31.2 | 32 | 31.8 | 13 |
| 46 | 11.6 | 30 | 11.8 | 14 | 91 | 32.1 | 37 | 32.7 | 20 |
| 47 | 11.9 | 31 | 12.1 | 15 | 92 | 33.2 | 41 | 33.7 | 27 |
| 48 | 12.1 | 31 | 12.4 | 16 | 93 | 34.4 | 46 | 34.9 | 36 |
| 49 | 12.4 | 32 | 12.8 | 17 | 94 | 35.7 | 51 | 36.3 | 10:47 |
| 50 | 12.7 | 33 | 13.1 | 18 | 95 | 37.5 | 5:56 | 38 | 11:00 |
| 51 | 13.0 | 33 | 13.3 | 20 | 96 | 39 | 6:07 | $39^1/_2$ | 11:15 |
| 52 | 13.3 | 34 | 13.7 | 21 | 97 | 41 | 18 | $41^1/_2$ | 11:33 |
| 53 | 13.6 | 35 | 14.0 | 22 | 98 | 44 | 32 | 44 | 11:56 |
| 54 | 13.9 | 35 | 14.3 | 24 | 99 | 47½ | 6:46 | 47 | 12:27 |
| 55 | 14.2 | 36 | 14.6 | 25 | 1.00 | 51½ | 7:02 | 50½ | 13:03 |

Calculated travel times of $PcP$, $ScP$ and $ScS$ for zero focal depth are given in the final columns of Tables 8, 9 and 10. Each table also shows the times assumed in calculating $PcP$, etc., for various depths as given in "Materials I". Residuals against these times for the available

Table 8.

Travel times of $PcP$ for zero focal depth. The residuals $R$ are from the deep focus earthquakes no. 30, 31, 34, 48, 101, 109 and 1932, May 1.

| Dist. degr. | Assumed "Materials" | $R$ sec. | Corrected travel time obs. | Calcul. travel time |
|---|---|---|---|---|
| 0 | 8:38 | | | 8:34 |
| 5 | 8:38 | | | 8:35 |
| 10 | 8:39 | | | 8:39 |
| 15 | 8:42 | | | 8:45 |
| 20 | 8:50 | | | 8:52 |
| 25 | 9:00 | | | 9:02 |
| 30 | 9:13 | 1 | 9:14 | 9:15 |
| 35 | 9:27 | 2 | 9:29 | 9:29 |
| 40 | 9:43 | 2 | 9:45 | 9:44 |
| 45 | 10:00 | 2 | 10:02 | 10:00 |
| 50 | 10:19 | 1 | 10:20 | 10:17 |
| 55 | 10:39 | 1 | 10:40 | 10:37 |
| 60 | 10:59 | 0 | 10:59 | 10:57 |
| 65 | 11:20 | —4 ? | 11:16 ? | 11:17 |
| 70 | 11:41 | —5 ? | 11:36 ? | 11:39 |
| 75 | 12:02 | | | 12:01 |
| 80 | 12:23 | | | 12:23 |

Table 9.

Travel times of $ScP$ for zero focal depth. The residuals $R$ are from the deep focus earthquakes no. 101 and 1932, May 1.

| Dist. degr. | Assumed "Materials" | $R$ sec. | Corrected travel time | Calcul. travel time |
|---|---|---|---|---|
| 0 | 12:08 | | | 12:08 |
| 10 | 12:12 | | | 12:14 |
| 20 | 12:24 | | | 12:32 |
| 30 | 12:52 | 5 ? | 12:57 ? | 12:59 |
| 40 | 13:29 | 4 ? | 13:33 ? | 13:35 |
| 50 | 14:10 | 7 ? | 14:17 ? | 14:15 |
| 60 | 14:52 | | | 14:57 |

Table 10.

Residuals of $ScS$ in deep focus earthquakes and revised travel times $t$ of $ScS$ for zero focal depth. (min.:sec.). $t_0$ is the travel time for zero depth on which the calculations of the travel times for larger depths have been based[4]).

| Dist. degr. | Numbers of shocks used: 17; 66; 54 234/50 101; 228 — Depth in km 100–200 | 48; 170; 182; 186 209 — 300–400 | 30; 31; 34 54; 57; 109; 173 — 500–700 | Assumed residuals — 0 | Travel time assumed in 'Materials' | Corrected travel time of $ScS$ | Calcul. travel time of $ScS$ |
|---|---|---|---|---|---|---|---|
| 0 | | 0 | 3 | 1 | 15:38 | 15:39 | 15:41 |
| 5 | | 3 | | 3 | 15:41 | 15:44 | 15:43 |
| 10 | | —1 | 0 | 0 | 15:47 | 15:47 | 15:48 |
| 15 | | 5 | | 5 | 15:56 | 16:01 | 15:59 |
| 20 | 5 ? | 5 ? | 0 | 4 | 16:10 | 16:14 | 16:14 |
| 25 | | 5 | | 5 | 16:27 | 16:32 | 16:32 |
| 30 | 6 ? | 1 | 5 ? | 4 | 16:49 | 16:53 | 16:53 |
| 35 | 6 | | | 6 | 17:16 | 17:22 | 17:20 |
| 40 | | 2 ? | | 2 | 17:45 | 17:47 | 17:48 |
| 45 | 3 | 2 ? | | 3 | 18:14 | 18:17 | 18:16 |
| 50 | 6 | | —1 | 3 | 18:44 | 18:47 | 18:47 |
| 55 | | 5 ? | 4 | 4 | 19:15 | 19:19 | 19:20 |
| 60 | | | | 7 | 19:49 | 19:56 | 19:57 |
| 65 | 12 | 8 | 6 | 9 | 20:27 | 20:36 | 20:36 |
| 70 | 8 ? | 8 | | 8 | 21:06 | 21:13 | 21:13 |
| 75 | | 9 | 6 | 8 | 21:47 | 21:55 | 21:55 |

observations of deep-focus shocks are included; serial numbers of the shocks used refer to our catalogue[6]). The procedure in determining these residuals and applying them to find corrected travel times, also given in the tables, is similar to that described for $S$ in the preceding section. The agreement between the times corrected to correspond to the observations, and the calculated times in the last columns, is very good; this indicates that the assumed velocity distribution is a very close approximation. This confirms the result of "Seismic Waves II" that there is no necessity for assuming any discontinuity of the type suggested by Dahm.

## V. Epicentral times of $P$ and $S$.

When a deep-focus earthquake is observed at stations near the epicenter, a small extrapolation gives valuable data on the travel times of $P$ and $S$ along a vertical ray. For this purpose the focal depth must be known with precision; this requires a fairly large shock, so that good instances are not numerous. All observed shocks which we have found useful in this way are listed in Table 11. The serial number, epicenter, origin time, and depth, as well as the lettering indicating quality of determination, are taken from our catalogue[6]. We have used no shocks to which a letter C had been assigned for either epicenter, origin time, or depth. The shock of July 25, 1932 has been examined since the publication of our catalogue, with the results shown in Table 11.

As might be expected, nearly all these shocks are in the Japanese area; the remaining three are in South America. With the following exceptions, we have used stations not over 1.3° distant from the epicenter: No. 195, stations Toyooka 0.7°, Osaka 1.7°, Kobe 1.8°; No. 11, La Paz 2.6°; No. 209, Vladivostok 2.8°. For the other two South American shocks the single stations are: No. 16, Montezuma 0.5°; No. 36, Sucre 1.0°.

Calculated differences between epicentral time and arrival time at the given distance have been subtracted from the observed arrival times to give the epicentral time. The quality of the result is given separately for $P$ and $S$ in the next to last column: A very precise, B good, C fair. This estimate depends on the quality of the shock determination, the number and reliability of the observing stations, and the agreement of the results. The quality has always been taken as C when only a single station was available. The times for $P_0$ and $S_0$, when plotted against depth, fall on nearly smooth curves.

Table 12 contains travel times of $ScS$ (lettered $t$) extrapolated to the epicenter, for earthquakes selected and worked out in the same manner as for Table 11. For this purpose we have used stations out to much larger distances than for $P_0$ and $S_0$, since the travel time of $ScS$ changes comparatively slowly with distance. We have used stations out to 15°, at which distance $ScS$ is 19 seconds later than at the epicenter. Where one or more stations have recorded $S$, this has also been extrapolated to the epicenter, and $S_0$ has been entered in Table 12. The sum $t + S_0$ should be a constant independent of focal depth; the several values in the table are in good agreement. The same constant can be determined by another method, the results of which are given in Table 13.

Table 11.

Travel time of $P$-waves ($P_0$) and of $S$-waves ($S_0$) in deep focus earthquakes from the focus to the epicenter (min.:sec.).

| No. | Day | Origin time | Coordinates of epicenter | Qual. | Number of stations | $P_0$ | $S_0$ | Qual. $P_0$ $S_0$ | Depth km |
|---|---|---|---|---|---|---|---|---|---|
| S 30 | 1929, July 26 | 22:48:16 | 35 ½ N 139 E | AAA | 4 | 0:07 | 0:14 | B C | 60 |
| 152 A | 1931, Jan. 10 | 16:07:48 | 39¾ N 140¾ E | ABB | 3 | 0:12 | 0:23 | C C | 80 |
| 155 | 1930, Dec. 13 | 17:22:50 | 43 N 142 ½ E | ABB | 4 | 0:16 | 0:25 | B C | 100 |
| 151 | 1929, Apr. 17 | 18:34:12 | 36 ½ N 141 E | ABA | 3 | 0:11 | 0:19 | C C | 100 |
| 16 | 1934, June 24 | 5:59:34 | 22 S 68.6 W | BAA | 1 | 0:18 | | C | 100 |
| 154 | 1931, March 29 | 17:51:52 | 42¾ N 143¾ E | AAB | 3 | 0:11 | 0:22 | C C | 120 |
| 152 | 1931, Jan. 9 | 1:45:40 | 39¾ N 140¾ E | AAA | 5 | 0:20 | 0:33 | A B | 140 |
| 11 | 1928, Sept. 21 | 13:27:05 | 15 S 70 ½ W | BBA | 1 | 0:35 | | C | 250 |
| 194 | 1931, June 2 | 2:37:52 | 36 N 137 ½ E | AAA | 5 | 0:34 | 1:00 | A A | 260 |
| 209 | 1931, Feb. 20 | 5:33:24 | 44.3 N 135 ½ E | AAA | 1 | 0:49 | 1:23 | C C | 350 |
| 193 | 1926, July 26 | 18:54:50 | 35 ½ N 135 ½ E | BAA | 3 | 0:45 | 1:20 | B B | 360 |
| — | 1932, July 25 | 8:42:39 | 35 ½ N 135 ½ E | AAA | 11 | 0:46 | 1:22 | A A | 360 |
| 189 | 1931, June 29 | 16:43:17 | 34 N 136 ½ E | AAA | 5 | 0:47 | 1:23 | A A | 380 |
| 195 | 1927, Jan. 15 | 14:31:16 | 36¼ N 134¼ E | AAB | 3 | 0:51 | 1:32 | B B | 420 |
| 36 | 1928, Jan. 5 | 21:46:13 | 19 ½ S 64 W | BBB | 1 | 1:06 | 2:02 | C C | 640 |

The procedure is to plot $S_0$ from Table 11 against depth, and to read the curve for selected depths; these times appear under $S_0$ in Table 13. The same procedure applied to Table 12 gives times for $ScS$ entered under $t$ in Table 13; the corresponding sums appear in the last column. Combining these results with the values of $t + S_0$ found in Table 12, we have adopted $15^m\,38^s$ as the value of this constant. This gives a travel time for $S$ along a vertical path between the core and the surface of the earth of $7^m\,49^s$; the calculated value (Table 7) is $7^m\,50^s$. Subtracting the observed values of $t$ from $15^m\,38^s$ gives a series of values for $S_0$, available even when $S$ is not observed. These results appear in the last column of Table 12; they furnish additional data for $S_0$, which combine very well with those of Table 11, and extend the observed smooth curve.

A similar method can be applied to find the travel time of longitudinal waves along an entire diameter of the earth; this constant is equal to $P_0 + t'$, where $t'$ is the extrapolated arrival time of $P'$ at the anticenter. This is done in Table 14, where $P_0$ is taken from curves based on Table 11, while $t'$ is similarly derived from the data of the

Table 12.

Travel time $t$ of $ScS$ and $S_0$ of $S$ to the epicenter in deep focus earthquakes (min:sec.).

| No. | Day | Origin time | Coordinates of epicenter | Depth km. | Qual. of shock | Number of stations | $t$ | Qual. of $t$ | $S_0$ | $t+S_0$ | Qual. of $t+S_0$ | 15:38 minus $t$ |
|---|---|---|---|---|---|---|---|---|---|---|---|---|
| 101 | 1934, May 1 | 7:04:56 | 3½ N 97½ E | 145 | ABA | 1 | 15:09 | C | | | | 0:29 |
| 17 | 1933, Oct. 25 | 23:28:16 | 23 S 66.7 W | 220 | AAA | 1 | 14:41 | C | | | | 0:57 |
| 194 | 1931, June 2 | 2:37:52 | 36 N 137½ E | 260 | AAA | 4 | 14:38 | B | 1:00 | 15:38 | B | 1:00 |
| 139 | 1936, Dec. 1 | 6:09:15 | 30 N 129 E | 270 | BBB | 3 | 14:34 | B | | | | 1:04 |
| 211 | 1932, Sept. 23 | 14:22:11* | 44¾ N 138 E* | 300 | AAA | 23 | 14:33 | A | (1:15) | 15:48 | C | 1:05 |
| 207 | 1932, Nov. 13 | 4:47:00 | 43¾ N 137 E | 320 | AAA | 24 | 14:22 | A | (1:16) | 15:38 | C | 1:16 |
| 209 | 1931, Feb. 20 | 5:33:24 | 44.3 N 135½ E | 350 | AAA | 20 | 14:19 | A | 1:23 | 15:42 | C | 1:19 |
| — | 1932, July 25 | 8:42:39 | 35½ N 135½ E | 360 | AAA | 8 | 14:14 | A | 1:22 | 15:36 | A | 1:24 |
| 192 | 1929, June 2 | 21:38:34 | 34½ N 137¼ E | 360 | AAA | 5 | 14:18 | A | | | | 1:20 |
| 182 | 1933, Sept. 2 | 16:41:08 | 29 N 138.8 E | 410 | AAA | 7 | 14:10 | A | | | | 1:28 |
| 183 | 1932, Apr. 4 | 19:16:31 | 29.1 N 138.8 E | 410 | AAA | 10 | 14:13 | A | | | | 1:25 |
| 186 | 1928, March 29 | 5:06:03 | 31.7 N 138.2 E | 410 | AAA | 11 | 14:06 | B | | | | 1:32 |
| 173 | 1933, March 11 | 19:32:39 | 26½ N 140½ E | 510 | ABB | 21 | 13:48 | A | | | | 1:50 |
| 114 | 1936, May 19 | 7:22:26 | 5¾ S 112¾ E | 610 | AAA | 1 | 13:34 | C | | | | 2:04 |
| 40 | 1936, Jan. 14 | 14:12:13 | 29 S 62½ W | 620 | AAA | 1 | 13:36 | C | | | | 2:02 |
| 34 | 1933, Aug. 29 | 14:52:36 | 10.9 S 69½ W | 650 | AAA | 1 | 13:28 | C | | | | 2:10 |
| 131 | 1930, Nov. 8 | 3:22:40 | 4 N 122½ E | 670 | ABB | 1 | 13:21 | C | | | | 2:17 |
| 109 | 1934, June 29 | 8:25:17 | 6¾ S 123¾ E | 720 | AAA | 1 | 13:09 | C | | | | 2:29 |

* Data revised

Table 13.

Travel time $S_0$ of transverse waves for the path focus-epicenter and $t$ for $ScS$ to the epicenter in deep focus earthquakes. The values are taken from curves based on observations. Data in parentheses are interpolated.

| Depth km. | $S_0$ | $t$ | $S_0+t$ |
|---|---|---|---|
| 250 | 0:58 | 14:40 | 15:38 |
| 300 | (1:08) | 29 | (37) |
| 350 | 18 | 19 | 37 |
| 400 | 28 | 10 | 38 |

Table 14.

Travel time $P_0$ of longitudinal waves for the path focus-epicenter and $t'$ for the path focus-anticenter in deep focus earthquakes; the values are taken from curves based on observations. Data in parentheses are interpolated. The times are given in min.:sec.

| Depth km. | $P_0$ | $t'$ | $P_0+t'$ |
|---|---|---|---|
| 100 | 0:14 | 20:00 | 20:14 |
| 150 | 21 | 19:53 | 14 |
| 200 | (28) | 47 | (15) |
| 250 | 34 | (40) | (14) |
| 300 | (40) | 33 | (13) |
| 350 | 45 | (28) | (13) |
| 400 | 50 | (23) | (13) |

following Table 15. We have only one instance of a deep-focus shock for which $P$ has been observed close enough to the epicenter to give $P_0$, and also $P'$ has been observed at great distance. This is No. 16; Montezuma, distant 0.5°, reports a time which gives $0^m\,18^s$ for $P_0$ while seven stations from 158° to 177° report times for $P'$ which give $t'$ as about $19^m\,58^s$; adding, $P_0 + t' = 20^m\,16^s$ (quality C). Combining this individual value with the results of Table 14, we have adopted $20^m\,14^s$ as the value of the constant. In the latter columns of Table 15 this has been used to derive additional values for $P_0$. These are in good agreement with those of Table 11. In finding $t'$, a wide range of epicentral distances has been used, since the time of $P'$ changes by only about $20^s$ from 140° to 180°, so that the extrapolation to 180° is very accurate.

Still another method for determining $P_0$ is based on the theoretical result $P_0 = {}^1/_2 D$, where $D$ is the interval $pP' - P'$ near 180°. $D$ can be determined with considerable accuracy; observed values of $D$ are given in Table 16. If the values in the column headed ${}^1/_2 D$ are really

Table 15.

Travel times $t'$ of $P'$-waves between the hypocenter and the anti-center of deep focus earthquakes (min.:sec.).

| No. | Day | Origin time | Coordinates of epicenter | Depth km. | Qual. of shock | Number of stations | $t'$ | Qual. of $t'$ | 20:14 minus $t'$ |
|---|---|---|---|---|---|---|---|---|---|
| 16 | 1934, June 24 | 5:59:34 | 22 S 68.6 W | 100 | BAA | 7 | 19:58 | B | 0:16 |
| 24 | 1927, Apr. 14 | 6:23:34 | 32 S 69 ½ W | 110 | BAA | 5 | 20:01 | B | 0:13 |
| 26 | 1934, March 1 | 21:45:25 | 40 S 72 ½ W | 120 | AAB | 3 | 19:57 | C | 0:17 |
| 135 | 1927, Apr. 13 | 13:44:14 | 16 N 120 ½ E | 140 | ABB | 2 | 19:55 | C | 0:19 |
| 23 | 1927, Nov. 26 | 12:53:58 | 24 ½ S 67 W | 180 | AAA | 4 | 19:50 | B | 0:24 |
| 17 | 1933, Oct. 25 | 23:28:16 | 23 S 66.7 W | 220 | AAA | 5 | 19:44 | A | 0:30 |
| 48 | 1935, Jan. 1 | 13:21:00 | 17 ½ S 174 ½ W | 300 | BAA | 4 | 19:33 | B | 0:41 |
| 207 | 1932, Nov. 13 | 4:47:00 | 43¾ N 137 E | 320 | AAA | 1 | 19:31 | C | 0:43 |
| 50 | 1928, Sept. 12 | 1:20:00 | 31 S 180 | 500 | BCC | 11 | 19:16 | C | 0:58 |
| 60 | 1935, July 29 | 7:38:53 | 20¾ S 178 W | 510 | AAA | 3 | 19:13 | C | 1:01 |
| 54 | 1934, Oct. 10 | 15:42:06 | 23 ½ S 180 | 540 | AAB | 7 | 19:09 | B | 1:05 |
| 57 | 1933, Sept. 6 | 22:08:29 | 21 ½ S 179¾ W | 600 | BAA | 7 | 19:04 | C | 1:10 |
| 40 | 1936, Jan. 14 | 14:12:13 | 29 S 62 ½ W | 620 | AAA | 6 | 19:09 | B | 1:05 |
| 34 | 1933, Aug. 29 | 14:52:36 | 11 S 69 ½ W | 650 | AAA | 4 | 18:58 | B | 1:16 |
| 30 | 1935, Dec. 14 | 1:31:13 | 9 ½ S 70 ½ W | 650 | AAA | 8 | 19:00 | A | 1:14 |
| 61 | 1931, Apr. 3 | 23:19:18 | 20 S 179¾ E | 680 | BAA | 9 | 18:58 | B | 1:16 |
| 109 | 1934, June 29 | 8:25:17 | 6¾ S 123¾ E | 720 | AAA | 4 | 18:52 | A | 1:22 |

Table 16.

Difference $D$ in travel time between $pP'$ and $P'$ at the anti-center and travel time $t'$ of $P'$ there in deep focus earthquakes (min.:sec.).

| No. | Coordinates of epicenter | Depth km | Qual. of shock | Number of stations | $D$ | Qual. of $D$ | ½ $D$ | $t'$ | $t'$ + ½ $D$ | Qual. |
|---|---|---|---|---|---|---|---|---|---|---|
| 17 | 23 S 66.7 W | 220 | AAA | 5 | 0:56 | C | 0:28 | 19:44 | 20:12 | C |
| 48 | 17 ½ S 174 ½ W | 300 | BAA | 13 | 1:14 | A | 0:37 | 19:33 | :10 | B |
| 60 | 20¾ S 178 W | 510 | AAA | 13 | 1:58 | B | 0:59 | 19:13 | :12 | C |
| 54 | 23 ½ S 180 W | 540 | AAB | 19 | 2:11 | B | 1:05 ½ | 19:09 | :14 ½ | B |
| 57 | 21 ½ S 179¾ W | 600 | BAA | 10 | 2:23 | A | 1:11 ½ | 19:04 | :15 ½ | C |
| 30 | 9 ½ S 70 ½ W | 650 | AAA | 9 | 2:29 | B | 1:14 ½ | 19:00 | :14 ½ | B |
| 34 | 11 S 69 ½ W | 650 | AAA | 7 | 2:24 | A | 1:12 | 18:58 | :10 | B |
| 31 | 9 ½ S 70 ½ W | 650 | AAA | 3 | 2:30 | C | 1:15 | — | — | — |
| 61 | 20 S 179¾ E | 680 | BAA | 8 | 2:34 | B | 1:17 | 18:58 | :15 | B |
| 109 | 6¾ S 123¾ E | 720 | AAA | 2 | 2:32 | C | 1:16 | 18:52 | :08 | C |

Table 17.

Travel times focus-epicenter for longitudinal and transverse waves in deep focus earthquakes, based on curves from observations of $P$ at the epicenter ($P_0$), $P'$ at the anticenter ($t'$), the difference $D = pP' - P'$ at the anticenter, $S$ at the epicenter ($S_0$) and $ScS$ at the epicenter ($t$). Data in parentheses are interpolated. Time in min.:sec.

| Depth km. | Longitudinal waves $P_0$ | 20:14 minus $t'$ | $^1/_2D$ | Calcul. from velocity | Transverse waves $S_0$ | 15:38 minus $t$ | calcul from velocity |
|---|---|---|---|---|---|---|---|
| 100 | 0:14 | 0:14 | | 0:13.9 | 0:25 | | 0:24.4 |
| 150 | 21 | 20 | | 20.1 | 36 | | 35.5 |
| 200 | (27) | 27 | | 26.3 | (47) | (0:47) | 46.6 |
| 250 | 33 | 33 | 0:32 | 32.4 | 58 | 58 | 57.5 |
| 300 | (39) | 40 | 37 | 38.3 | (1:08) | 1:08 | 1:08.1 |
| 350 | 44 | (45) | (43) | 43.9 | 18 | 18 | 18.5 |
| 400 | 49 | (50) | (49) | 49.4 | 28 | 28 | 28.5 |
| 450 | | (55) | (54) | 54.7 | | (38) | 38.2 |
| 500 | | 1:00 | 59 | 59.8 | | 48 | 47.6 |
| 550 | | 05 | 1:05 | 1:04.8 | | (56) | 56.8 |
| 600 | | 10 | 09 | 09.6 | | 2:05 | 2:05.7 |
| 650 | | 14 | 14 | 14.1 | | 14 | 14.4 |
| 700 | | 19 | 18 | 18.8 | | 22 | 22.9 |

equal to $P_0$, we should have $t' + {}^1/_2D =$ constant. The results, in the next to last column, agree so well with the adopted value of $20^m 14^s$ that there is little doubt that the values $^1/_2D$ actually do represent $P_0$.

Table 17 gives the values for $P_0$ and $S_0$ found in these various ways. Other columns show the values calculated from the velocity distribution. The agreement is very good, which shows that the present travel times and velocities are highly accurate.

## VI. Observed travel times of $P'$.

Residuals for the observed cases of $P'$ in our deep-focus shocks are given in Table 18. These residuals are with reference to Table 7 of "Materials I." Table 18 (a) gives residuals for the principal phase of the $P'$ group; except at the shortest distances, these are small. The second line of Table 18 (c) gives the corresponding residuals for $P_2'$. Table 18 (b) represents a number of early readings which probably belong to two distinct groups; the observations from 105° to 115° are almost exclusively from BENIOFF short-period vertical instruments; while those from 125° to 135° are also taken in part from long-period GALITZIN vertical instruments. These early readings are probably not due to longitudinal waves approximately following the laws of geometrical optics; a phenomenon of diffraction is presumably involved.

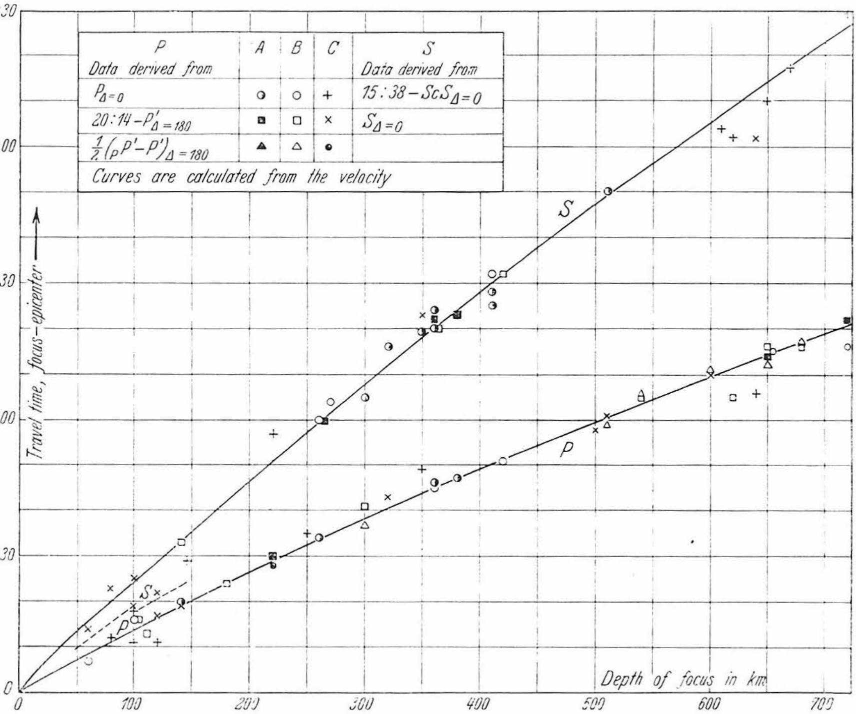


Fig. 1. Travel times focus-epicenter in min.:sec. as a function of the depth of focus. The barred line at short distances separates the observations for $P$ from those for $S$.

The extension of the main $P'$ phase to distances as short as 110° is not due to diffraction, as formerly supposed. These readings can be represented by a revision of the velocity distribution within the core. (See section VIII below.)

In Table 19 the column headed A contains travel times of $P'$ for zero depth, on which Table 7 of "Materials I" has been based. B contains corrections based on the residuals in Table 18 (a); C gives corrected travel times for $P'$, which have been smoothed after application

Table 18.
Residuals of $P'$ in deep focus earthquakes, travel times $t_0$ for zero depth on which the travel times for larger depth have been based, and corrected travel times $t$ for zero depth (min.:sec.).

| Dist. degr. | Serial numbers of shocks: 16; 24; 28 May 1, 1932 | 72 107 255 | 17; 23 Hindu-Kush | 48 83 211 | 51 54 60 | 40 57 114 | 29/31; 34 | 109 | assumed residual |
|---|---|---|---|---|---|---|---|---|---|
| | Depth in km. 100 | 150 | 200 | 350 | 520 | 610 | 650 | 720 | 0 |
| | a) Main phase of $P'$ | | | | | | | | |
| 110 | 7 | 11 | | | | | | 2 | 7 |
| 115 | | 4 | | 8 | 8 ? | —3 | | —1 | 3 |
| 120 | —4 | 0 | | . 3 | —1 | —6 | 0 | —2 | —2 |
| 125 | —4 | —3 | 0 | 0 | —1 | —3 | | —2 | —2 |
| 130 | 0 | —2 | 0 | —4 | 0 | | | | —1 |
| 135 | | 0 | | —1 | 0 | —2 | | 1 | 0 |
| 140 | 5 | —6 | 3 | | | 0 | 0 | 2 | 1 |
| $142^1/_2$ | 5 | —1 | | | | 0 | 2 | 1 | 2 |
| 145 | 2 | 0 | | —2! | 1 ? | 0 | 0 | 1 | —1 |
| 150 | —2 | 0 | —1 | —4 | —4! | —4 | —3 | | —3 |
| 155 | 0 | —1 | 1 | —2 | —2! | 0 | 0 | 1 | —1 |
| 160 | 0 | 0 | 0 | —2 | 1 | 0 | | | 0 |
| 180 | From table 15 | | | | | | | | 0 |

b) Small early phases, recorded only by instruments with high magnification

| Dist. | Depth in km 100 | 150 | 350 | 520 | 610 | 720 | assumed | $t_0$ | $t$ |
|---|---|---|---|---|---|---|---|---|---|
| 105 | —13 | | | | | | —13 | 18:10 | 17:57 |
| 110 | —15 | | | | | —17 | —16 | 27 | 18:11 |
| 115 | | —11 | | | | | —11 | 42 | 31 |
| 125 | | —14 | | | | | —14 | 19:05 | 51 |
| 130 | | —18 | —14 | | | | —16 | 15 | 59 |
| 135 | | —13 ? | | —12 | —17 | | —16 | 22 | 19:06 |

c) $P_2'$ (from shocks no. 26, 30, 48, 54, 57, 60).

| Dist. degr. | 148 | 150 | 152 | 154 | 156 | 158 | 160 |
|---|---|---|---|---|---|---|---|
| Corr. obs. | —14 | —15 | —15 | —14 | —14 | —15 | —14 |
| $t_0$ | 20:01 | 20:10 | 20:20 | 20:30 | 20:40 | 20:50 | 20:59 |
| $t$ | 19:47 | 19:55 | 20:05 | 20:16 | 20:26 | 20:35 | 20:45 |

Table 19.

Travel times of $P'$ (main phase) in minutes:seconds. A: travel time for zero depth on which the calculated values for deep foci have been based[4]; B: observed correction (table 18); C assumed values after smoothing; $1/v$:reciprocal values of the apparent velocity in seconds/degree; $i$ is the corresponding angle of incidence of longitudinal waves at the surface of the core. $\sin i = 0.22779/v$. The last four columns give the angular distance of the path $\theta_M$ in the mantle, $\theta_C$ in the core and the corresponding travel times.

| Dist. degr. | A | B | C | $1/v$ | $\sin i$ | $\theta_M$ degr. | $t_M$ min:sec | $\theta_c$ degr. | $t_c$ min:sec |
|---|---|---|---|---|---|---|---|---|---|
| 106 | 18:17 | (10) | 18:27 | 2.55 | (0.581) | | | | |
| 108 | 24 | (9) | 32 | 2.45 | (558) | 28.9 | 9:12 | 79.1 | 9:20 |
| 110 | 30 | 7 | 37 | 2.35 | 538 | 27.5 | 9:10 | 82.5 | 9:27 |
| 112 | 37 | 5 | 41 | 2.25 | 513 | 26.2 | 9:07 | 86.6 | 9:35 |
| 114 | 42 | 4 | 46 | 2.15 | 490 | 24.8 | 9:04 | 89.2 | 9:42 |
| 116 | 48 | 2 | 50 | 2.05 | 467 | 23.5 | 9:01 | 92.5 | 9:49 |
| 118 | 53 | 0 | 54 | 2.0 | 456 | 23.0 | 8:59 | 95.0 | 9:55 |
| 120 | 59 | —2 | 58 | 2.0 | 456 | 23.0 | 8:59 | 97.0 | 9:58 |
| 122 | 19:04 | —2 | 19:02 | 2.0 | 456 | 23.0 | 59 | 99.0 | 10:02 |
| 124 | 07 | —2 | 06 | 2.0 | 456 | 23.0 | 59 | 101.0 | 06 |
| 126 | 12 | —2 | 10 | 1.95 | 444 | 22.2 | 58 | 103.8 | 12 |
| 128 | 16 | —2 | 14 | 1.9 | 433 | 21.5 | 57 | 106.5 | 17 |
| 130 | 19 | —1 | 18 | 1.85 | 421 | 20.8 | 56 | 109.2 | 22 |
| 132 | 22 | —1 | 21 | 1.75 | 399 | 19.7 | 54 | 112.3 | 27 |
| 134 | 25 | 0 | 25 | 1.65 | 376 | 19.2 | 52 | 114.8 | 33 |
| 136 | 28 | 0 | 28 | 1.6 | 364 | 17.9 | 50 | 118.1 | 38 |
| 138 | 30 | 1 | 31 | 1.6 | 364 | 17.9 | 50 | 120.1 | 41 |
| 140 | 31 | 1 | (34) | (1.6) | (364) | | | | |
| 142 | 32 | 2 | (37) | (1.6) | (364) | | | | |
| 144 | 38 | 0 | (41) | (1.6) | (364) | | | | |
| 146 | 45 | —1 | (44) | (1.6) | (364) | | | | |
| 148 | 50 | —3 | 47 | 1.6 | 364 | 17.9 | 8:50 | 130.1 | 10:57 |
| 150 | 53 | —3 | 50 | 1.6 | 364 | 17.9 | 50 | 132.1 | 11:00 |
| 152 | 57 | —3 | 53 | 1.6 | 364 | 17.9 | 50 | 134.1 | 04 |
| 154 | 59 | —2 | 57 | 1.55 | 353 | 17.3 | 49 | 136.7 | 08 |
| 156 | 20:01 | —1 | 20:00 | 1.5 | 342 | 16.7 | 48 | 139.3 | 12 |
| 158 | 03 | 0 | 03 | 1.45 | 330 | 16.1 | 47 | 141.9 | 16 |
| 160 | 05 | 0 | 05 | 1.35 | 308 | 14.9 | 46 | 145.1 | 19 |
| 162 | 07 | 1 | 08 | 1.15 | 262 | 12.6 | 43 | 149.4 | 25 |
| 164 | 08 | 2 | 10 | 0.85 | 194 | 9.2 | 39 | 154.8 | 31 |
| 166 | 10 | 2 | 11 | 0.6 | 148 | 7.0 | 37 | 159.0 | 34 |
| 168 | 11 | 1 | 12 | 0.4 | 103 | 4.8 | 36 | 163.2 | 36 |
| 170 | 11 | 1 | 13 | 0.25 | 080 | 3.8 | 35 | 166.2 | 37 |
| 180 | 14 | 0 | 14 | 0.0 | 000 | 0.0 | 34 | 180.0 | 40 |

of the residuals in B. The following columns will be discussed in section VIII.

The two last columns of Table 18 (b), and the two last lines of Table 18 (c), give corrected and smoothed travel times for the early arrivals and for $P_2'$, respectively.

## VII. Observations of *SKS*.

The travel time curves for *SKS* and *S* intersect at about 82°. This divides observations of *SKS* into two classes: those at shorter

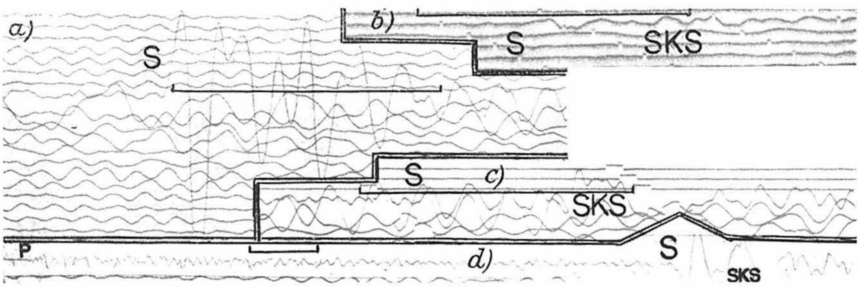


Fig. 2. Records showing the appearance of *SKS* near the focal point. The length of one minute is indicated in each seismogram. a) 1933, February 23, 8$^h$, Chile, recorded at Pasadena, distance $70^1/_2$°, long period Benioff, N-S. *SKS* should be close to *ScS*, about one minute after *S*, if it exists. b) 1928, November 20, 20$^h$, Chile, recorded at Pasadena, distance $72^1/_2$°, long period Wood-Anderson, E-W. c) 1933, March 2, 17$^h$, off Japan, recorded at Tinemaha, distance $73^1/_2$°, short period Wood-Anderson, N-S. d) 1936, July 13, 11$^h$, Chile, recorded at Pasadena, distance 76°, Benioff strain seismograph, N-S.

distances, where *SKS* follows *S*, and those at greater distances, where it precedes.

At the shorter distances the beginning of *SKS* is usually obscured by *S*, which makes it difficult to construct accurate tables for *SKS*. However, it is not unlikely that *SKS* has a focal point in this range*).

*) In a recent paper[11]) it has been shown by one of us that focal points near the beginning of SKS are to be considered. Two cases have been discussed: a) that the travel time curve of SKS begins with a branch extending to increasing distance, and b) to descreasing distance. In a letter, Miss I. LEHMANN points out that only case a) is possible; case b) requires that the second derivative of a travel time curve has a finite value for zero distance, while actually it seems to be zero. It is intended to discuss this problem elsewhere. The results for SKS found in this paper (Table 24) belong to case a) with two focal points, the first of which is very close to the beginning of SKS.

To determine the position of this focus we have investigated the seismograms available at Pasadena. It appears that from 73° to 77° a large phase follows *S* after about the interval to be expected for *SKS*. The phenomenon is best studied in normal shocks; it can be observed on the seismograms of deep-focus shocks, but additional care is then required to avoid confusion with *sS*, etc. The distance at which the focus occurs decreases with increasing depth of focus, so that for very deep shocks the phenomenon is to be expected several degrees earlier.

A very clear case is provided by the Japanese earthquake of March 2, 1933. The seismogram of the long-period strain instrument at Pasadena (distant 75°) has been published elsewhere[12]). The large phase there indicated as *S* is really *SKS*; the true *S*, about 1 minute earlier, is smaller, but plainly recorded. Figure 2 of the present paper shows further examples of this type, which make it highly probable that a large and sharp focus of *SKS* exists at distances close to 75°.

Beyond 82° the observed travel times of *SKS* in deep shocks have been used in the same manner as described above for *P* and *P'*. The residuals with respect to Table 28 of "Materials I" appear in the present

Table 20.

Residuals of *SKS* in deep focus earthquakes in seconds.

| Dist. degr. | Numbers of shocks used: 61, 109, 131 | 29; 30, 34; 38, 40 | 51; 54, 60, 173 | 83, 182, 186 | 128, 192, 209 | 11, 48, 170 | 17; 23, 241, 246/9 | 9; 101, 135, 255 | 16, 26, 150 | assumed |
|---|---|---|---|---|---|---|---|---|---|---|
| | Average depth of focus: 690 | 640 | 520 | 400 | 360 | 270 | 220 | 150 | 120 | 0 |
| 80 | | | | | | | | —2 | | —2 ? |
| 85 | | —3 | 1 | 0 | —4 | | 0 | —3 | | —1 |
| 90 | | —3 | 2 | —4 | —3 | —2 | 0 | 1 | 1 | —1 |
| 95 | | —3 | 0 | —2 | —2 | 0 | 1 | 4 | 5 | 0 |
| 100 | —5 | —6 | | —1 | —2 | | 1 | 3 | 5 | —1 |
| 105 | —4 | —6 | | —3 | —8 ? | | | 2 | 2 | —3 |
| 110 | | —5 | —2 | —4 | | 0 | | —3 | —2 | —3 |
| 115 | —4 | —6 | | —5 | | | —3 | —4 | —3 | —4 |
| 120 | —5 | | —5 | | | —7 ? | —5 | | | —5 |

125°—150° Data for all depths show residuals in general between —2 and —7 seconds, average about —5 seconds.

Table 21.

Travel times of *SKS* in minutes:seconds. A: travel times for zero depth on which the calculated values for deep foci have been based[4]); B: observed corrections (table 20): C: assumed values after smoothing; $1/v$:reciprocal values of the apparent velocity in seconds/degree; $i$ is the corresponding angle of incidence of transverse waves at the surface of the core. $\sin i = 0.1205/v$ (the values are smoothed). $\theta_M$ and $\theta_C$ are the angular distances of the paths in the mantle and the core, respectively, $t_M$ and $t_C$ the corresponding travel times.

| Dist. degr. | A | B | C | $1/v$ | $\sin i$ | $\theta_M$ degr. | $t_M$ min.:sec. | $\theta_c$ degr. | $t_c$ min.:sec. |
|---|---|---|---|---|---|---|---|---|---|
| 80 | 22:29 | —2 | 22:27 | 7.0 | 0.844 | 55.0 | 19:21 | 25.0 | 3:06 |
| 82 | 42 | —2 | 41 | 6.8 | 819 | 51.9 | 19:00 | 30.1 | 3:41 |
| 84 | 55 | —1 | 54 | 6.5 | 789 | 48.5 | 18:38 | 35.5 | 4:16 |
| 86 | 23:08 | —1 | 23:07 | 6.3 | 759 | 45.6 | 18:18 | 40.4 | 4:49 |
| 88 | 21 | —1 | 19 | 6.1 | 735 | 43.2 | 18:05 | 44.8 | 5:14 |
| 90 | 32 | —1 | 31 | 5.9 | 711 | 41.0 | 17:53 | 49.0 | 5:38 |
| 92 | 44 | —1 | 43 | 5.7 | 687 | 39.0 | 42 | 53.0 | 6:01 |
| 94 | 55 | 0 | 54 | 5.5 | 663 | 37.0 | 32 | 57.0 | 6:22 |
| 96 | 24:06 | 0 | 24:05 | 5.4 | 645 | 35.7 | 25 | 60.3 | 6:40 |
| 98 | 18 | —1 | 16 | 5.2 | 627 | 34.4 | 18 | 63.6 | 6:58 |
| 100 | 27 | —1 | 26 | 5.0 | 603 | 32.6 | 09 | 67.4 | 7:17 |
| 102 | 37 | —2 | 36 | 4.8 | 578 | 30.9 | 00 | 71.1 | 7:36 |
| 104 | 47 | —3 | 45 | 4.6 | 554 | 29.4 | 16:51 | 74.6 | 7:54 |
| 106 | 56 | —3 | 54 | 4.5 | 536 | 28.3 | 46 | 77.7 | 8:08 |
| 108 | 25:06 | —3 | 25:03 | 4.4 | 530 | 27.9 | 44 | 80.1 | 8:19 |
| 110 | 16 | —3 | 12 | 4.4 | 530 | 27.9 | 44 | 82.2 | 8:28 |
| 112 | 25 | —4 | 20 | 4.4 | 530 | 27.9 | 44 | 84.1 | 8:36 |
| 114 | 34 | —4 | 29 | 4.4 | 530 | 27.9 | 44 | 86.1 | 8:45 |
| 116 | 43 | —4 | 38 | 4.3 | 518 | 27.2 | 41 | 88.8 | 8:57 |
| 118 | 51 | —5 | 46 | 4.1 | 494 | 25.7 | 35 | 92.3 | 9:11 |
| 120 | 59 | —5 | 54 | 3.6 | 434 | 22.1 | 22 | 97.9 | 9:32 |
| 122 | 26:06 | —5 | 26:01 | 2.8 | 343 | 17.2 | 07 | 104.8 | 9:54 |
| 124 | 11 | —5 | 06 | 2.5 | 295 | 14.6 | 15:58 | 109.4 | 10:08 |
| 126 | 15 | —5 | 11 | 2.4 | 289 | 14.3 | 57 | 111.7 | 14 |
| 128 | 21 | —5 | 15 | 2.4 | 289 | 14.3 | 57 | 113.7 | 18 |
| 130 | 25 | —5 | 20 | 2.4 | 289 | 14.3 | 57 | 115.7 | 23 |
| 132 | 30 | —5 | 25 | 2.3 | 283 | 14.0 | 56 | 118.0 | 29 |
| 134 | 34 | —5 | 30 | 2.3 | 277 | 13.7 | 56 | 120.3 | 34 |
| 136 | 39 | —5 | 34 | 2.2 | 271 | 13.4 | 55 | 122.6 | 36 |
| 138 | 44 | —5 | 39 | 2.1 | 253 | 12.5 | 53 | 125.5 | 46 |

Tabelle 21 (Continued).

| Dist. degr. | A | B | C | $1/\bar{v}$ | sin $i$ | $\theta_M$ degr. | $t_M$ min:sec. | $\theta_c$ degr. | $t_c$ min:sec. |
|---|---|---|---|---|---|---|---|---|---|
| 140 | 48 | —5 | 43 | 1.9 | 229 | 11.3 | 51 | 128.7 | 52 |
| 142 | 52 | —5 | 46 | 1.8 | 211 | 10.4 | 49 | 131.6 | 57 |
| 144 | 55 | —5 | 50 | 1.6 | 193 | 9.5 | 47 | 134.5 | 11:03 |
| 146 | 58 | —5 | 53 | 1.4 | 169 | 8.2 | 45 | 137.8 | 08 |
| 148 | 27:00 | —5 | 55 | 1.2 | 145 | 7.0 | 44 | 141.0 | 11 |
| 150 | 02 | —5 | 57 | | | | | | |

Table 20. In Table 21, column A gives travel times of *SKS* for zero depth, as assumed in computing the tables of "Materials I"; column B contains residuals from Table 20, and column C gives the corrected and smoothed travel times of *SKS* for zero focal depth. The remaining columns are for use in the following section.

## VIII. Travel times through the core (*K*).

In "Seismic Waves II" we have described how travel times between points on the surface of the core can be derived from observations at the surface of the earth. This procedure has been applied to the corrected travel times for $P'$ ($= PKP$) and *SKS*, as given in preceding sections. (Tables 19 and 21.) In Table 19 sin $i$ is the angle of incidence of longitudinal waves ($P$) at the exterior surface of the core, calculated from the reciprocal apparent velocities given in the preceding column. The two following columns give the corresponding angular distances and travel times through the mantle, derived from Table 7. Subtracting these values from the corresponding angular distances and travel times for $P'$ leaves as remainders the angular distances and travel times for $K$ between points on the surface of the core; these will be found in the two last columns. The observed travel times for *SKS* have been used in a similar way, and the results for $K$ will be found in the last two columns of Table 21.

The two sets of results for $K$ agree within the limits of error. These have been compared, combined, and adjusted to represent the observations, all this work being carried out under the hypothesis presented by the writers in a recent paper[13]). It is there shown that the observed waves which had previously been referred to a "diffracted" $P'$ are better accounted for as $P'$ waves normally refracted through the core.

Table 22.

Travel times $t$ between points on the surface of the core, reciprocals $1/v$ of the apparent velocity in seconds per degree; sines of the angles of incidence $i_P$ and $i_S$ in the mantle at the surface of the core; angular distances $\theta_{MP}$ and $\theta_{MS}$ for the arc between the surface of the earth and the surface of the core and corresponding travel times $t_{MP}$ and $t_{MS}$ as a function of the angular distance of the arc inside the core ($\theta_C$). The index "$P$" refers to longitudinal waves, the index "$S$" to transverse waves. The distances are given in degrees, the times in min.:sec.

$\sin i_P = 0.22779/v$; $\sin i_S = 0.1205/v$.

| $\theta_C$ | $t$ | $1/v$ | $\sin i_S$ | $\theta_{MS}$ | $t_{MS}$ |
|---|---|---|---|---|---|
| 0 | 0:00 | 8.1 | 0.976 | 43.8 | 11:48 |
| 2 | 16 | 8.1 | 974 | 43.5 | 11:42 |
| 4 | 32 | 8.1 | 970 | 41.5 | 11:33 |
| 6 | 48 | 8.0 | 964 | 40.3 | 11:22 |
| 8 | 1:04 | 7.9 | 952 | 37.7 | 11:03 |
| 10 | 20 | 7.7 | 928 | 34.6 | 10:34 |
| 12 | 35 | 7.6 | 916 | 33.3 | 10:24 |
| 14 | 50 | 7.5 | 904 | 32.2 | 10:15 |
| 16 | 2:05 | 7.3 | 880 | 30.1 | 10:00 |
| 18 | 19 | 7.1 | 856 | 28.3 | 9:46 |
| 20 | 33 | 6.9 | 831 | 26.6 | 9:35 |
| 22 | 47 | 6.8 | 819 | 25.9 | 30 |
| 24 | 3:01 | 6.7 | 807 | 25.2 | 26 |
| 26 | 14 | 6.7 | 802 | 25.0 | 23 |
| 28 | 27 | 6.6 | 795 | 24.6 | 21 |
| 30 | 41 | 6.5 | 783 | 23.9 | 17 |
| 32 | 53 | 6.4 | 771 | 23.4 | 13 |
| 34 | 4:06 | 6.3 | 762 | 22.9 | 11 |
| 36 | 19 | 6.3 | 756 | 22.6 | 09 |
| 38 | 31 | 6.2 | 750 | 22.3 | 07 |
| 40 | 44 | 6.2 | 743 | 22.0 | 05 |
| 42 | 56 | 6.1 | 738 | 21.7 | 03 |
| 44 | 5:08 | 6.1 | 732 | 21.5 | 9:01 |
| 46 | 21 | 6.0 | 723 | 21.1 | 8:59 |
| 48 | 32 | 5.9 | 711 | 20.4 | 57 |
| 50 | 44 | 5.8 | 699 | 20.0 | 54 |
| 52 | 55 | 5.7 | 687 | 19.5 | 51 |
| 54 | 6:07 | 5.5 | 663 | 18.6 | 46 |
| 56 | 18 | 5.4 | 651 | 18.1 | 44 |
| 58 | 28 | 5.3 | 639 | 17.7 | 41 |

Table 22 (Continued).

| $\theta_C$ | $t$ | $1/\bar{v}$ | $\sin i_P$ | $\sin i_S$ | $\theta_{MP}$ | $\theta_{MS}$ | $t_{MP}$ | $t_{MS}$ |
|---|---|---|---|---|---|---|---|---|
| 60 | 6:39 | 5.2 | | 0.630 | | 17.3 | | 8:40 |
| 62 | 49 | 5.2 | | 623 | | 17.1 | | 38 |
| 64 | 59 | 5.1 | | 618 | | 16.9 | | 37 |
| 66 | 7:10 | 5.1 | | 614 | | 16.8 | | 36 |
| 68 | 20 | 5.1 | | 610 | | 16.6 | | 36 |
| 70 | 30 | 5.0 | | 605 | | 16.4 | | 35 |
| 72 | 40 | 5.0 | | 600 | | 16.2 | | 34 |
| 74 | 50 | 4.9 | | 590 | | 15.8 | | 32 |
| 76 | 8:00 | 4.8 | | 578 | | 15.5 | | 30 |
| 78 | 09 | 4.7 | | 566 | | 15.1 | | 28 |
| 80 | 19 | 4.6 | | 554 | | 14.7 | | 26 |
| 82 | 28 | 4.5 | | 542 | | 14.3 | | 24 |
| 84 | 37 | 4.4 | (1.00) | 530 | (51.5) | 13.9 | (7:04) | 22 |
| 86 | 45 | 4.3 | 0.979 | 518 | 43.7 | 13.6 | 6:31 | 21 |
| 88 | 54 | 4.2 | 957 | 506 | 38.5 | 13.3 | 6:04 | 19 |
| 90 | 9:02 | 4.1 | 934 | 494 | 34.9 | 12.9 | 5:48 | 17 |
| 92 | 10 | 4.0 | 911 | 482 | 32.1 | 12.5 | 5:38 | 16 |
| 94 | 18 | 3.8 | 866 | 458 | 28.4 | 11.8 | 5:20 | 14 |
| 96 | 25 | 3.6 | 820 | 434 | 25.4 | 11.1 | 5:10 | 11 |
| 98 | 32 | 3.4 | 775 | 410 | 23.0 | 10.4 | 5:02 | 09 |
| 100 | 39 | 3.3 | 752 | 398 | 21.8 | 10.0 | 4:58 | 08 |
| 102 | 46 | 3.14 | 715 | 378 | 20.2 | 9.5 | 52 | 06 |
| 104 | 52 | 3.11 | 708 | 375 | 19.9 | 9.4 | 51 | 06 |
| 106 | 58 | 3.10 | 706 | 374 | 19.8 | 9.4 | 51 | 06 |
| 108 | 10:04 | 3.09 | 705 | 373 | 19.8 | 9.4 | 51 | 06 |
| 110 | 10 | 3.09 | 704 | 372 | 19.7 | 9.4 | 50 | 06 |
| 112 | 17 | 3.09 | 703 | 372 | 19.6 | 9.4 | 50 | 06 |
| 114 | 23 | 3.08 | 702 | 371 | 19.6 | 9.3 | 50 | 06 |
| 116 | 29 | 3.08 | 701 | 371 | 19.6 | 9.3 | 50 | 06 |
| 118 | 35 | 3.08 | 701 | 371 | 19.6 | 9.3 | 50 | 05 |
| 120 | 41 | 3.08 | 701 | 371 | 19.6 | 9.3 | 50 | 05 |
| 122 | 47 | 3.08 | 700 | 371 | 19.6 | 9.3 | 50 | 05 |
| 124 | 53 | 3.07 | 699 | 370 | 19.6 | 9.3 | 50 | 05 |
| 126 | 11:00 | 3.07 | 699 | 370 | 19.5 | 9.3 | 50 | 05 |
| 128 | 11:06 | 3.07 | 698 | 370 | 19.5 | 9.3 | 50 | 05 |
| 130 | 11:12 | 3.07 | 698 | 370 | 19.5 | 9.3 | 50 | 05 |

Table 22 (Continued).

| $\theta_C$ | $t$ | $1/v$ | $\sin i_P$ | $\sin i_S$ | $\theta_{MP}$ | $\theta_{MS}$ | $t_{MP}$ | $t_{MS}$ |
|---|---|---|---|---|---|---|---|---|
| 128 | 11:06 | 2.90 | 0.661 | 0.349 | 18.0 | 8.8 | 4:46 | 8:04 |
| 126 | 11:00 | 2.70 | 615 | 325 | 16.3 | 8.1 | 41 | 01 |
| 124 | 10:55 | 2.50 | 570 | 301 | 14.8 | 7.4 | 38 | 7:59 |
| 122 | 51 | 2.37 | 540 | 286 | 13.9 | 7.1 | 35 | 58 |
| 120 | 46 | 2.30 | 524 | 277 | 13.4 | 6.8 | 34 | 58 |
| 115 | 35 | 2.17 | 494 | 261 | 12.5 | 6.5 | 32 | 57 |
| 110 | 24 | 2.12 | 482 | 255 | 12.2 | 6.3 | 31 | 57 |
| 105 | 14 | 2.08 | 474 | 251 | 12.0 | 6.2 | 31 | 56 |
| 100 | 10:03 | 2.06 | 469 | 248 | 11.8 | 6.2 | 30 | 56 |
| 95 | 9:53 | 2.03 | 463 | 245 | 11.7 | 6.1 | 30 | 56 |
| 90 | 43 | 2.01 | 458 | 242 | 11.5 | 6.0 | 30 | 56 |
| 88 | 39 | 2.00 | 456 | 241 | 11.4 | 5.9 | 30 | 56 |
| 90 | 9:43 | 2.00 | 455 | 241 | 11.4 | 5.9 | 30 | 56 |
| 95 | 9:53 | 1.98 | 451 | 239 | 11.3 | 5.9 | 29 | 56 |
| 100 | 10:03 | 1.97 | 448 | 237 | 11.2 | 5.8 | 29 | 55 |
| 105 | 10:13 | 1.94 | 442 | 234 | 11.0 | 5.8 | 29 | 55 |
| 110 | 22 | 1.91 | 435 | 230 | 10.8 | 5.7 | 28 | 55 |
| 115 | 32 | 1.88 | 428 | 227 | 10.6 | 5.6 | 28 | 55 |
| 120 | 41 | 1.84 | 419 | 222 | 10.4 | 5.5 | 28 | 55 |
| 125 | 50 | 1.80 | 410 | 217 | 10.1 | 5.4 | 27 | 55 |
| 130 | 59 | 1.72 | 392 | 207 | 9.7 | 5.1 | 26 | 54 |
| 135 | 11:07 | 1.61 | 376 | 194 | 9.0 | 4.8 | 25 | 54 |
| 140 | 15 | 1.46 | 333 | 176 | 8.2 | 4.3 | 24 | 53 |
| 145 | 22 | 1.31 | 298 | 158 | 7.2 | 3.8 | 22 | 52 |
| 150 | 28 | 1.06 | 241 | 128 | 5.7 | 3.1 | 21 | 52 |
| 155 | 32 | 0.70 | 159 | 084 | 3.8 | 2.0 | 19 | 51 |
| 160 | 35 | 0.48 | 109 | 058 | 2.5 | 1.4 | 18 | 51 |
| 165 | 37 | 0.34 | 077 | 041 | 1.8 | 1.0 | 18 | 51 |
| 170 | 38 | 0.24 | 055 | 029 | 1.3 | 0.7 | $17\frac{1}{2}$ | 50 |
| 180 | 40 | 0.00 | 000 | 000 | 0.0 | 0.0 | 17 | 50 |

The final revised travel times for $K$ appear in Table 22. This table also contains the reciprocal apparent velocity at the surface of the core; with the corresponding exterior angles of incidence, and travel times through the mantle, for both longitudinal and transverse waves. These data, together with those of Table 7, suffice for the calculation of travel times for all waves passing through the core.

Fig. 3. Wave paths and wave fronts of direct longitudinal waves in the earth.

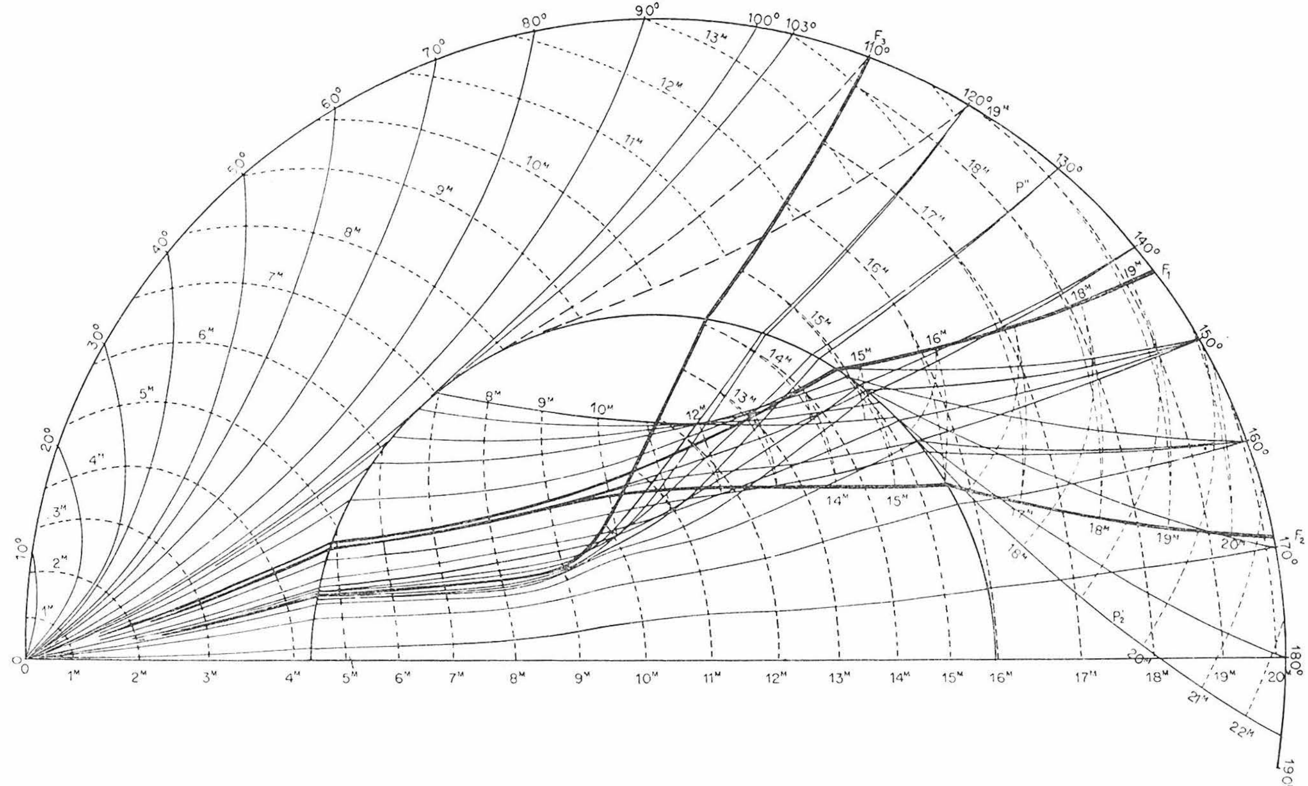

In constructing Table 22, the times at short distances have been adjusted so as to represent the observed focus of *SKS*.

## IX. Calculated travel times of core waves.

Table 23 gives times for the various branches of $P'$, calculated for zero focal depth from the data of the preceding section; these are compared with observed times as taken from Tables 18 and 19.

Seismograms showing large amplitudes for $P''$ have been published elsewhere[13]). Figure 4 here shows two additional examples.

Figure 3 is drawn to show the complicated rays and wave-fronts consequent on the revised travel time data for the core.

Table 24 gives observed and calculated times for *SKS*. As for $P'$, the order is that of decreasing angle of incidence. There are four turning points, dividing the travel time curve into five branches. The second of these is the branch discussed in section VII above, with which the strong focus near 75° is associated. The last two branches are produced by the peculiar conditions within the core, and correspond to the similar complications in $P'$.

Table 23.

Observed and calculated travel times (min.:sec.) of longitudinal waves which pass through the core, for zero focal depth.

| a) $P_2'$ | | | b) $P'$ and reversed segment | | c) $P''$ | | |
|---|---|---|---|---|---|---|---|
| Dist. degr. | travel times obs. | travel times calc. | Dist. degr. | travel times calc. | Dist. degr. | travel times obs. (tab. 19) | travel times calc. |
| | | | 142½ | 19:30 | 110 | 18:37 | 18:37 |
| 180 | (see | 22:19 | 145 | 19:38 | 115 | 18:48 | 18:47 |
| 175 | table | 21:53 | 150 | 19:53 | 120 | 18:58 | 18:57 |
| 170 | 18) | 21:28 | 155 | 20:08 | 125 | 19:08 | 19:07 |
| 165 | | 21:04 | 160 | 20:23 | 130 | 19:18 | 19:16 |
| | | | 165 | 20:38 | | | |
| 160 | 20:45 | 20:40 | 169 | 20:51 | 135 | 19:27 | 19:26 |
| 155 | 20:21 | 20:18 | | | 140 | (19:34) | 19:35 |
| 150 | 19:55 | 19:56 | 160 | 20:26 | 145 | (19:42) | 19:44 |
| 145 | | 19:38 | 150 | 20:02 | 150 | 19:50 | 19:52 |
| 142½ | (19:32) | 19:30 | 140 | 19:39 | 155 | 19:58 | 19:59 |
| | | | 130 | 19:18 | | | |
| | | | 120 | 18:58 | 160 | 20:05 | 20:06 |
| | | | 110 | 18:37 | 165 | 20:10 | 20:11 |
| | | | | | 170 | 20:13 | 20:13 |
| | | | | | 180 | 20:14 | 20:14 |

Table 25 gives times for $SKP$. The fact that this phase has a branch at short distances, similar to $P''$, has been discussed elsewhere[13]). The best available series of observations of this branch are those for the earthquake of 1935 May 14, $23^h$; they are reproduced in Table 26. See also Figure 4.

Tables 27 and 28 give calculated times for $PKKP$ and $SKKP$. No new observations are available for comparison; the data at hand

Table 24. Observed and calculated travel times (min.:sec.) of $SKS$ for zero focal depth.

| Dist. degr. | travel times obs. | travel times calc. | Dist. degr. | travel times obs. | travel times calc. |
|---|---|---|---|---|---|
| 87½ | | 23.6 | 140 | | 26:56 |
| | | | 130 | | 26:34 |
| 89 | | 23.7 | 120 | | 26:12 |
| | | | 110 | | 25:51 |
| 85 | (see | 23:21 | | | |
| 80 | table | 22:36 | 100 | | 25:31 |
| 75 | 21) | 21:55 | | | |
| | | | 105 | | 25:41 |
| 73½ | | 21:43 | 110 | | 25:51 |
| | | | 115 | | 26:01 |
| 75 | | 21:55 | 120 | | 10 |
| 80 | (22:27) | 22:29 | | | |
| 85 | 23:01 | 23:01 | 125 | | 20 |
| 90 | 23:31 | 23:32 | 130 | | 29 |
| | | | 135 | 26:32 | 38 |
| 95 | 24:00 | 24:00 | 140 | 26:43 | 47 |
| 100 | 24:26 | 24:26 | | | |
| 105 | 24:49 | 24:51 | 145 | 26:52 | 26:55 |
| 110 | 25:12 | 25:14 | 150 | (26:57) | 27:03 |
| 115 | 25:33 | 25:35 | 160 | | 15 |
| 120 | 25:54 | 25:54 | 180 | | 20 |
| 125 | 26:09 | 26:11 | | | |
| 130 | 26:20 | 26:27 | | | |
| 135 | other | 26:42 | | | |
| 140 | branch | 26:56 | | | |
| 148½ | | 27:21 | | | |

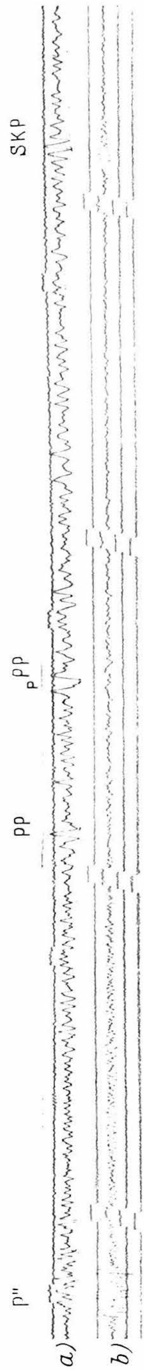


Fig. 4. Seismograms showing $P''$-and $SKP$ at a distance of about 119°, a) 1935, May 14, $23^h$; epicenter near 59° S. 26½° W, depth about 150 km., recorded at Pasadena, short period Benioff vertical. b) 1937, September 8, $0^h$; about same epicenter and depth, recorded at Riverside, short period Benioff vertical.

agree with the calculations within the limits of error. *SKKP* usually is not well observed.

The phase *SKKS* is very strong at large distances; it is often reported as *S*. Calculation at first indicaded that the large wave is so late as more nearly to fit *SKKKS* (section XXIV, Seismic Waves I; section IX, Seismic Waves II); however, this now appears less probable. In Table 29 observed times for this phases from deep-focus earthquakes are assembled, reduced to zero depth by means of the travel times in Table 30 of "Materials I." It is evident that there are relatively large differences between the several shocks, which is chiefly due to the very

Table 25.
Calculated travel times $t$ (min.:sec.) of *SKP* or *PKS* for zero focal depth.

| Dist. degr. | $t$ | Dist. degr. | $t$ | Dist. degr. | $t$ |
|---|---|---|---|---|---|
| 149½ | (24:03) | | | 105 | 22:05 |
| 145 | 23:42 | 158¾ | 24:07 | 110 | 14 |
| 140 | 23:18 | | | 115 | 24 |
| 135 | 22:56 | 150 | 23:41 | 120 | 33 |
| | | 140 | 23:17 | | |
| 131½ | 22:43 | 130 | 22:55 | 125 | 43 |
| | | 120 | 22:34 | 130 | 52 |
| 135 | 22:54 | 110 | 22:14 | 135 | 23:02 |
| 140 | 23:10 | | | 140 | 11 |
| 145 | 23:25 | 104¼ | 22:04 | | |
| 150 | 23:40 | | | 145 | 20 |
| 155 | 23:55 | | | 150 | 28 |
| | | | | 160 | 42 |
| | | | | 180 | 47 |

Table 26.
Observed travel times of *SKP*, reduced to approximately zero focal depth by adding 30 seconds, for the South Atlantic earthquake of 1935, May 14, 23:23:10, depth of focus about 150 km., and calculated travel times for zero focal depth.

| Station | Dist. degr. | Travel time obs. | Travel time calc. | Station | Dist. degr. | Travel time obs. | Travel time calc. |
|---|---|---|---|---|---|---|---|
| Philadelphia . | 105½ | 22:16 | 22:06 | Tinemaha . | 121½ | 22:38 | 22:36 |
| Strasbourg . | 111½ | 29 | 17 | Berkeley . . | 124½ | 33 | 42 |
| Praha . . . | 114 | 32 | 22 | Honolulu . | 130 | 40 | 52 |
| Pasadena . . | 119 | 33 | 31 | Manila . . | 130 | 38 | (40) |
| Riverside . . | 119 | 29 | 31 | Seattle . . | 132½ | 47 | 48 |
| Santa Barbara | 121 | 29 | 35 | Hongkong . | 134 | 52 | 51 |

long period and indefinite beginning of these waves, which probably leads to somewhat late readings. Accordingly, the agreement between observed times and the calculated times, as given in Table 30 of the

Table 27.

Calculated travel times of *PKKP* for zero focal depth. Asterisks indicate the earliest times of arrival for a given distance where there are several branches.

| Dist. degr. | Travel time of *PKKP* | Travel time of *PKKP-P* | Dist. degr. | Travel time of *PKKP* | Travel time of *PKKP-P* |
|---|---|---|---|---|---|
| 86 | (31.4) | | 70 | 31:38 | |
| 100 | 30:29 | | 90 | 30:39 | |
| 105 | 30:03 | | 100 | 30:26 | |
| 110 | 29:39 | | 120 | 29:42 | |
| 115 | 29:17 | | 140 | 28:59 | |
| 118 | 29:07* | | 161 | 28:18 | |
| (120) | (28:58*) | | | | |
| | | | 150 | 28:39* | |
| 115 | 29:17* | 14:20 | 140 | 28:59* | |
| 110 | 29:33* | 14:59 | 130 | 29:18* | |
| 105 | 29:48* | 15:36 | 120 | 29:37 | |
| 100 | 30:03* | 16:13 | 110 | 29:56 | |
| 95 | 30:19* | 16:52 | | | |
| | | | 100 | 30:14 | |
| 90 | 30:34 | | 90 | 30:32* | 17:27 |
| 85 | 30:49 | | 80 | 30:50* | 18:35 |
| 80 | 31:04 | | 70 | 31:06* | 19:48 |
| 70 | 31:36 | | 60 | 31:22* | 21:09 |
| | | | 0 | 31:54 | |
| 61 | 32:04 | | | | |

Table 28.

Calculated travel times of *SKKP* or *PKKS* for zero focal depth.

| Dist. degr. | Travel time | Dist. degr. | Travel time |
|---|---|---|---|
| $126^1/_2$ | 32.7 | 71 | 35:19 |
| 132 | 32:09 | 100 | 34:04 |
| | | 130 | 32:58 |
| 125 | 32:33 | | |
| 120 | 32:49 | 168 | 31:43 |
| 115 | 33:04 | | |
| 110 | 33:19 | 130 | 32:56 |
| 100 | 33:50 | 100 | 33:52 |
| | | 0 | 35:27 |

Table 29. Travel times of the strong phase of $SKKS$ in min.:sec.

| Shock No. | 255 | 43 | 48 | 50 | 54 | 52*) | 57 | 61 | 109 | Assumed |
|---|---|---|---|---|---|---|---|---|---|---|
| Depth km. | 150 | 180 | 300 | 500 | 540 | 600 | 600 | 680 | 720 | |
| Quality .. | BBB | BCC | BAA | BCC | AAB | BCB | BAA | BAA | AAA | |
| Dist. degr. | | | | | | | | | | |
| | | | | | a) As observed. | | | | | |
| 100 | | | | | | 23:05 | | 23:03 | | |
| 105 | | | 24:38 | | | 23:35 | | 23:36 | | |
| 110 | 25:34 | | 25:07 | | | 24:10 | | 24:04 | 23:56 | |
| 115 | 26:10 | | 25:40 | | | 24:40 | | 24:40 | 24:28 | |
| 120 | 26:46 | | 26:10 | | | 25:10 | | 25:12 | 25:00 | |
| 125 | 27:15 | | 26:40 | | | 25:42 | | | 25:28 | |
| 130 | 27:46 | | 27:10 | | | 26:16 | | | 26:00 | |
| 135 | 28:18 | | 27:40 | | 27:08 | 26:43 | | 26:48 | 26:31 | |
| 140 | | | 28:10 | | 27:35 | 27:11 | 27:38 | 27:18 | 27:02 | |
| 145 | | 29:20 | 28:40 | 28:13 | | 27:45 | 28:06 | 27:47 | 27:29 | |
| 150 | 29:50 | 29:46 | 29:10 | 28:40 | 28:30 | 28:10 | 28:28 | 28:17 | 27:58 | |
| 155 | | 30:10 | 29:40 | 29:10 | 28:56 | 28:36 | 28:54 | 28:45 | 28:27 | |
| 160 | | 30:30 | | 29:38 | 29:26 | | 29:20 | 29:14 | | |
| 165 | | 30:50 | | 30:06 | 29:51 | | | | | |
| | | | | | b) Reduced to zero depth. | | | | | |
| 100 | | | | | | 25:08 | | 25:17 | | (25:12) |
| 105 | | | 25:44 | | | 25:38 | | 25:50 | | 25:44 |
| 110 | 26:09 | | 26:13 | | | 26:13 | | 26:18 | 26:19 | 26:15 |
| 115 | 26:45 | | 26:46 | | | 26:43 | | 26:54 | 26:51 | 26:47 |
| 120 | 27:21 | | 27:16 | | | 27:13 | | 27:26 | 27:23 | 72:18 |
| 125 | 27:50 | | 27:46 | | | 27:45 | | | 27:52 | 27:49 |
| 130 | 28:21 | | 28:16 | | | 28:19 | | | 28:20 | 28:20 |
| 135 | 28:53 | | 28:46 | | 29:01 | 28:46 | | 29:02 | 28:51 | 28:52 |
| 140 | | | 29:16 | | 29:28 | 29:18 | 29:41 | 29:33 | 29:25 | 29:23 |
| 145 | | 30:04 | 29:46 | 29:58 | | 29:48 | 30:09 | 30:02 | 29:53 | 29:54 |
| 150 | 30:24 | 30:30 | 30:16 | 30:25 | 30:23 | 30:13 | 30:31 | 30:32 | 30:22 | 30:24 |
| 155 | | 30:54 | 30:46 | 30:55 | 30:49 | 30:39 | 30:57 | 31:00 | 30:51 | 30:53 |
| 160 | | 31:14 | | 31:23 | 31:19 | | 31:23 | 31:29 | | 31:22 |
| 165 | | 31:34 | | 31:51 | 31:46 | | | | | (31:48) |

*) This shock shows several impulses with increasing intensity. As origin time for the strong $SKKS$-waves 16:09:55 has been assumed. The origin time assumed by Brunner[14]) in a special investigation of this shock is 16:09:58. The origin time for the first motion found by the authors[6]) is 16:09:40.

Table 30.
Observed and calculated travel times (min.:sec.) of *SKKS* for zero focal depth.

| Dist. degr. | Travel times obs. | Travel times calc. | Dist. degr. | Travel times obs. | Travel times calc. | Dist. degr. | Travel times calc. |
|---|---|---|---|---|---|---|---|
| $87^{1}/_{2}$ | | 23.6 | 135 | 28:52 | 28:45 | 170 | 33:33 |
| | | | 140 | 29:23 | 29:15 | 160 | 34:17 |
| $92^{1}/_{2}$ | | 24.3 | 145 | 29:54 | 29:44 | 140 | 35:34 |
| | | | 150 | 30:24 | 30:12 | 120 | 36:36 |
| $89^{1}/_{4}$ | | 23.8 | | | | 100 | 37:35 |
| | | | 155 | 30:53 | 30:39 | | |
| 95 | | 24:29 | 160 | 31:22 | 31:05 | $81^{1}/_{2}$ | 38:34 |
| 100 | (25:12) | 25:03 | 165 | (31:48) | 31:31 | | |
| 105 | 25:44 | 25:36 | 170 | | 31:57 | 120 | 37.0 |
| 110 | 26:15 | 26:08 | | | | 150 | 35.9 |
| | | | 180 | | 32:46 | | |
| 115 | 26:47 | 26:40 | | | | 172 | 35.2 |
| 120 | 27:18 | 27:12 | | | | | |
| 125 | 27:49 | 27:43 | | | | 120 | 36.9 |
| 130 | 28:20 | 28:14 | | | | 80 | 38.0 |
| | | | | | | 0 | 39.0 |

present paper, must be considered as fairly good, although not altogether satisfactory.

Table 31 gives observed times for $P'P'$, $P'P'P'$, and $SKPP'$, and calculated times for the observed ranges. Tables 32, 33, 34 give calculated times for the complete theoretical ranges of these phases.

Table 35 gives calculated times for *SKSP*; and finally Table 36 contains calculated distances and times for the focal points of a number of complex phases.

## X. Wave velocities and elastic constants in the interior of the earth.

The travel times of $K$ given in Table 22 have been used to calculate the velocity distribution of waves in the core, using the formulae

$$\log r = 3.5375 - 0.0024127 \int \cosh q \, d\theta \qquad (\theta \text{ in degrees})$$

$$V = \frac{r \cdot 7.25}{3446 \cdot \sin i_S} = 0.002104 \, r/\sin i_S$$

where $i_S$ is the angle of exterior incidence of transverse waves at the core. These results are included in Table 37 (b).

Table 31.
Observed travel times of $P'P'$ and related waves reduced to zero focal depth and calculated values for zero focal depth. Distances in degrees, time in min.:sec.

a) $P'P'$.

| Dist. degr. | $P'P'$—O obs. | $P'P'$—O calc. | $P'P'—P$ obs. | $P'P'—P$ calc. |
|---|---|---|---|---|
| 55 | 39.9 | 39:51 | 30.2 | 30:15 |
| 60 | 39:40 | 39:44 | 29:27 | 29:31 |
| 65 | 39:28 | 39:30 | 28:40 | 28:47 |
| 70 | 39:18 | 39:16 | 28:00 | 27:58 |
| 75 | 39:00 | 39:00 | 27:15 | 27:14; 27:32 |
| 80 | 39:10 | 39:10 | 26:54 | 26:55 |
| 85 | 39:00 | 39:01 | 26:18 | 26:21 |
| 90 | 38:50 | 38:52 | 25:43 | 25:47 |

b) $P'P'P'$.

| Dist. degr. | $P'P'P'$—O obs. | $P'P'P'$—O calc. | $P'P'P'—P$ obs. | $P'P'P'—P$ calc. |
|---|---|---|---|---|
| 75 | 58:50 | 58:53 | 47:00 | 47:06 |
| 80 | 59:08 | 59:08 | 46:50 | 46:53 |
| 85 | 59:23 | 59:21 | 46:40 | 46:40 |
| 90 | 59.5 | 59:30 | 46.4 | 46:25 |

c) $SKPP'$.

| Dist. degr. | $SKPP'$—O obs. | $SKPP'$—O calc. |
|---|---|---|
| 75 | 42.8 | 42:47 |
| 80 | 42:30 | 42:32 |
| 85 | 42:18 | 42:16 |

For comparison, wave velocities, elastic constants, and density for various rocks are given in Table 37 (a). It should be noted that for sedimentary rocks the properties of different samples show considerable variation.

Tables 37 (b) gives velocities at various depths. Those for the mantle are taken from Table 6 of the present paper and 18 of Seismic Waves II; those for the core are calculated from Table 22. The table

Table 32.

Calculated travel times of $P'P'$ for zero focal depth. Asterisks indicate the earliest times of arrival for a given distance where there are several branches.

| Dist. degr. | Travel times of $P'P'$ | Travel times of $P'P'$-$P$ | Dist. degr. | Travel times of $P'P'$ | Travel times of $P'P'$-$P$ |
|---|---|---|---|---|---|
| 0 | 44:38 | | | | |
| 20 | 42:56 | | 140 | 37:14* | |
| 40 | 41:20 | | | | |
| 60 | 39:52 | | 130 | 37:34* | |
| | | | 120 | 37:54* | |
| 75 | 39:00* | 27:14 | 110 | 38:14* | 23:40 |
| | | | 100 | 38:33* | 24:43 |
| 70 | 39:16* | 27:58 | | | |
| 60 | 39:46 | | 90 | 38:52* | 25:47 |
| 50 | 40:16 | | 80 | 39:10* | 26:55 |
| 40 | 40:45 | | 70 | 39:27 | |
| | | | 60 | 39:44* | 29:31 |
| 22 | 41:42 | | 50 | 39:59* | 30:59 |
| | | | 40 | 40:12* | 32:30 |
| 60 | 40:04 | | | | |
| 80 | 39:18 | | 0 | 40:28 | 40:28 |
| 100 | 38:36 | | | | |

Table 33.

Calculated travel times of $P'P'P'$ for zero focal depth. Asterisks indicate the earliest times of arrival for a given distance where there are several branches.

| Dist. degr. | Travel times of $P'P'P'$ | Dist. degr. | Travel times of $P'P'P'$ | Travel times of $P'P'P'$-$P$ | Dist. degr. | Travel times of $P'P'P'$ | Travel times of $P'P'P'$-$P$ |
|---|---|---|---|---|---|---|---|
| | | | | | 0 | 56:54 | |
| 180 | 66:57 | | | | | | |
| 150 | 64:24 | $67^1/_2$ | 58:30* | 47:26 | 30 | 55:52* | |
| 120 | 62:00 | | | | | | |
| 110 | 61:15 | 70 | 58:37* | 47:19 | 0 | 56:54* | |
| | | 80 | 59:08* | 46:53 | | | |
| 100 | 60:31 | 90 | 59:39 | | 30 | 57:53 | |
| 90 | 59:48 | 120 | 61:09 | | 60 | 58:42* | 48:38 |
| 80 | 59:10 | | | | 90 | 59:30* | 46:25 |
| 70 | 58:38 | 147 | 63:33 | | 120 | 60:15* | |
| | | | | | 180 | 60:42 | |
| | | 90 | 60:04 | | | | |
| | | 30 | 57:56 | | | | |

also shows Poisson's constant

$$\sigma = \tfrac{1}{2}\left[1 - \frac{1}{(v_P/v_S)^2 - 1}\right]$$

and the elastic constants $\mu$ and $k$, together with the density and pressure as calculated by Bullen[15]).

Table 34.

Calculated travel times of $SKPP'$ (or $P'SKP$ or $PKSP'$ or $P'PKS$) for zero focal depth. Asterisks indicate the earliest times of arrival for a given distance where there are several branches.

| Dist. degr. | Travel time of $SKPP'$ | Travel time of $SKPP'$-$P$ | Dist. degr. | Travel time of $SKPP'$ | Travel time of $SKPP'$-$P$ | Dist. degr. | Travel time of $SKPP'$ | Travel time of $SKPP'$-$P$ |
|---|---|---|---|---|---|---|---|---|
| 23½ | 46:48 | | 80 | 42:32* | 30:17 | 120 | 41:31* | |
| 40 | 45:22 | | 70 | 43:03* | 31:45 | 110 | 41:50* | 27:16 |
| 50 | 44:39 | | 60 | 43:34 | | 100 | 42:08* | 28:18 |
| | | | | | | 90 | 42:27* | 29:22 |
| 60 | 43:56 | | 32 | 45:00 | | | | |
| 70 | 43:15 | | | | | 80 | 42:46 | |
| 80 | 42:35 | | 86 | 42:43 | | 70 | 43:03* | 31:45 |
| | | | | | | 60 | 43:20* | 33:07 |
| 86 | 42:13* | 29:27 | 145 | 40:44* | | 40 | 43:50* | 36:08 |
| | | | | | | 0 | 44:01 | |

Table 35.

Calculated travel times of $SKSP$ or $PSKS$ for zero focal depth.

| Dist. degr. | Travel time minutes | Dist. degr. | Travel time minutes |
|---|---|---|---|
| 132 | 31.9 | 150 | 33.8 |
| | | 155 | 34.3 |
| 126 | 31.1 | 160 | 34.8 |
| | | 170 | 35.7 |
| 130 | 31.5 | | |
| 135 | 32.1 | 180 | 36.6 |
| 140 | 32.7 | | |
| 145 | 33.3 | 145 | 39.4 |

Table 36.

Epicentral distance $D$ and travel time $t$ to the main focal points of some phases for zero focal depth. In the last column the direction of the two branches (to increasing distance or decreasing distance) is indicated.

| Phase | $D$ degr. | $t$ min. | direction of branches |
|---|---|---|---|
| *PKKKP* . . . . . . . . . . . . . . . | 21 | 38.6 | decr. dist. |
| *SKSP', P'SKS, SKPPKS, PKSSKP, SKPSKP, PKSPKS* . . . . . . . . | 97 | 45.4 | decr. „ |
| *SKSSKP, PKSSKS, SKPSKS, SKSPKS* | 110 | 48.5 | decr. „ |
| *ScSP, PScS* . . . . . . . . . . . . | 112 | 29.3 | incr. „ |
| | 115 | 29.6 | decr. „ |
| | 110 | 29.0 | incr. „ |
| *SKSSKS* . . . . . . . . . . . . . | $146^1/_2$ | 43.4 | incr. „ |
| *P'P'P'P'* . . . . . . . . . . . . . | 150 | 78.0 | incr. „ |
| *ScSSKP, PcSSKS, ScPSKS, SKPScS, PKSScS, ScSPKS, SKSPcS, SKSScP* | 151 | 39.0 | incr. „ |
| *ScSP', PcPSKS, PcSSKP, PcSPKS, ScPSKP, ScPPKS, P'ScS, SKSPcP, SKPScP, PKSScP, PKSPcS, SKPPcS* | 161 | 35.7 | incr. „ |
| *PcPPKS, PcPSKP, ScPP', P'ScP, PcSP', P'ScP, SKPPcP, PKSPcP* . . . . . | 172 | 32.5 | incr. „ |
| *PcPP', P'PcP* . . . . . . . . . . . | 178 | 29.2 | decr. „ |

Table 37.

Velocity of longitudinal waves ($v_P$) and of transverse waves ($v_S$) in km./sec., Poisson's ratio $\sigma$, density $\varrho$ in g./cm.$^3$, rigidity $\mu$ (in $10^{-12}$ dynes/cm$^2$) bulk modulus $k$ (in $10^{-12}$ dynes/cm.$^2$) and pressure $p$ (in $10^{-12}$ dynes/cm.$^2$) as a function of depth (in km.). $\varrho$ and $p$ after Bullen[15]). It has been assumed that in the core the coefficient of rigidity is small compared with the bulk modulus.

a) Some characteristic data for rocks; all values show noticeable differences for different samples.

| Material | depth | $v_P$ | $v_S$ | $\sigma$ | $\varrho$ | $\mu$ | $k$ |
|---|---|---|---|---|---|---|---|
| Young sediments . | 0.1 | 1 | | | 2.6 | | |
| Pleistocene sandstone . . . . . . | 0.1 | 2 | | | 2.7 | | |
| | 1.0 | $2\frac{1}{2}$ | | | | | |
| Triassic gypsum | 0.1 | 3 | | | 2.7 | | |
| | 2 | $4\frac{1}{2}$ | | | | | |
| Devonian sandstone | 1 | 4 | | | 2.8 | | |

Tabelle 37 (Continued)

| Depth | $v_P$ | $v_S$ | $\sigma$ | $\varrho$ | $\mu$ | $k$ | $p$ |
|---|---|---|---|---|---|---|---|
| Ordovician limestone | | 0.1 | 5 | | | 2.8 | |
| | | 1 | 6 | | | | |
| Granite | | 0.1 | 5 | (2½) | (0.33) | 2.7 | 0.2 | 0.4 |
| Norite | | 0.1 | 6¼ | 3½ | 0.27 | 2.8 | 0.3 | 0.7 |

b) Data for the interior of the earth; the first line refers to the "granitic layer" in the continents, the second and third lines to characteristic continental layers; these data differ in different regions.

| Depth | $v_P$ | $v_S$ | $\sigma$ | $\varrho$ | $\mu$ | $k$ | $p$ |
|---|---|---|---|---|---|---|---|
| 5 | 5.5 | 3.2 | 0.25 | 2.9 | 0.3 | 0.5 | 0.0014 |
| 20 | 5.8 | 3.4 | 24 | 3.0 | 0.4 | 0.6 | 0055 |
| 40 | 7.0 | 4.1 | 24 | 3.1 | 0.5 | 0.8 | 011 |
| 40 | 7.9 | 4.5 | 26 | 3.3 | 0.7 | 1.1 | 017 |
| 100 | 8.0 | 4.5 | 27 | 3.4 | 0.7 | 1.2 | 03 |
| 200 | 8.1 | 4.6 | 28 | 3.5 | 0.8 | 1.3 | 06 |
| 300 | 9.0 | 4.8 | 30 | 3.6 | 0.8 | 1.8 | 10 |
| 400 | 9.6 | 5.1 | 30 | 3.6 | 0.9 | 2.1 | 13 |
| 500 | 10.0 | 5.3 | 30 | 4.2 | 1.2 | 2.6 | 17 |
| 600 | 10.4 | 5.6 | 29 | 4.3 | 1.3 | 3.0 | 22 |
| 700 | 10.8 | 5.9 | 29 | 4.4 | 1.5 | 3.1 | 26 |
| 800 | 11.2 | 6.1 | 29 | 4.4 | 1.7 | 3.3 | 30 |
| 900 | 11.4 | 6.3 | 29 | 4.5 | 1.8 | 3.4 | 35 |
| 1000 | 11.4 | 6.4 | 28 | 4.6 | 1.9 | 3.5 | 39 |
| 1200 | 11.7 | 6.5 | 0.28 | 4.7 | 2.0 | 3.8 | 0.48 |
| 1400 | 12.1 | 6.6 | 28 | 4.8 | 2.1 | 4.2 | 58 |
| 1600 | 12.4 | 6.8 | 28 | 4.9 | 2.3 | 4.5 | 67 |
| 1800 | 12.5 | 6.9 | 28 | 5.0 | 2.4 | 4.7 | 77 |
| 2000 | 12.8 | 7.0 | 28 | 5.1 | 2.5 | 5.1 | 87 |
| 2200 | 13.2 | 7.0 | 30 | 5.2 | 2.5 | 5.7 | 97 |
| 2400 | 13.3 | 7.1 | 30 | 5.3 | 2.7 | 5.8 | 1.07 |
| 2600 | 13.5 | 7.1 | 31 | 5.4 | 2.7 | 6.2 | 18 |
| 2800 | 13.8 | 7.3 | 31 | 5.5 | 2.9 | 6.5 | 29 |
| 2920 | 13.7 | 7.25 | 31 | 5.6 | 2.9 | 6.4 | 36 |

Tabelle 37 (Continued).

| Depth | $v_P$ | $v_S$ | $\sigma$ | $\varrho$ | $\mu$ | $k$ | $p$ |
|---|---|---|---|---|---|---|---|
| 2920 | 7.4 | | | 9.7 | | $5^1/_2$ | 36 |
| 3000 | 7.9 | | | 9.8 | | 6 | 44 |
| 3200 | 8.6 | | | 10.1 | | 7 | 64 |
| 3400 | 8.9 | | | 10.4 | | 8 | 84 |
| 3600 | 9.2 | | | 10.7 | | 9 | 2.03 |
| 3800 | 9.3 | | | 10.9 | | 9 | 22 |
| 4000 | 9.4 | | | 11.1 | | 10 | 39 |
| 4200 | 9.5 | | | 11.3 | | 10 | 56 |
| 4400 | 9.8 | Assumed to be small | Assumed to be about 0.5 | 11.5 | Assumed to be small | 11 | 73 |
| 4600 | 10.0 | | | 11.6 | | 11 | 87 |
| 4800 | 10.0 | | | 11.7 | | 12 | 3.00 |
| 5000 | 10.2 | | | 11.8 | | 12 | 12 |
| 5100 | 10.6 | | | 11.9 | | 13 | 17 |
| 5200 | 11.0 | | | 11.9 | | 14 | 22 |
| 5400 | 11.0 | | | 12.0 | | 14 | 31 |
| 5600 | 11.0 | | | 12.1 | | 14 | 38 |
| 5800 | 10.9 | | | 12.1 | | 14 | 44 |
| 6000 | 10.9 | | | 12.2 | | 14 | 48 |
| 6366 | 10.8 | | | 12.2 | | 14 | 51 |

## Summary.

Travel times and velocities of seismic waves have been revised, using observational data from deep-focus earthquakes. Travel times for zero focal depth are given for all important phases. The revised velocity distribution closely represents the observations of *PcP*, *PcS*, and *ScS*, as well as the arrival times of waves at the epicenter and anticenter. The revision includes a reinterpretation of the observations of *P'* and *SKS*. Velocities and elastic constants are tabulated as functions of depth.

## References.

1. B. Gutenberg and C. F. Richter, "On seismic waves (first paper)" Gerlands Beitr. Geophysik **43** (1934) 56—133.
2. Do. (second paper). Ibid. **45** (1935) 280—360.
3. Do. (third paper). Ibid. **47** (1936) 73—131.
4. B. Gutenberg and C. F. Richter, "Materials for the study of deep-focus earthquakes". Bull. Seism. Soc. Amer. **26** (1936) 341—390.

5. Do. (second paper). Ibid. **27** (1937) 157—183.
6. B. Gutenberg and C. F. Richter, "Depth and geographical distribution of deep-focus Earthquakes". Bull. Geol. Soc. Amer. **49** (1937) 249—288.
7. H. Jeffreys, "The ellipticity correction of the *P* table". Mthly Not. Roy. Astron. Soc., Geophys. Suppl., **4** (1937) 165—184. See especially p. 183.
8. H. Jeffreys, "Further corrections to the *P*, *S* and *SKS* tables". Ibid. **4** (1937) 225—250. See especially p. 246.
9. B. Gutenberg, "Travel time curves at small distances and wave velocities in Southern California. Gerlands Beitr. Geophysik **35** (1932) 6—50.
10. See reference [7] p. 182 and reference [8] p. 249.
11. B. Gutenberg, "On focal points of *SKS*". Bull. Seism. Soc. Amer. **28** (1938) 197—200.
12. H. Benioff, "A linear strain seismograph". Bull. Seism. Soc. Amer. **25** (1935) 283—309. See especially figure 14 on p. 302.
13. B. Gutenberg and C. F. Richter, "*P′* and the earth's core". Mthly Not. Roy. Astron. Soc., Geophys. Suppl., **4** (1938) 363—372.
14. G. J. Brunner, "The deep earthquake of May 26, 1932 near the Kermadec Islands". Gerlands Beitr. Geophysik **53** (1938) 1—64.
15. K. E. Bullen, "Note on the density and pressure inside the earth". Transact. R. Soc. of New Zealand **67** (1937) 122—124.